A Catalogue of 20th and 21st Century Droughts for the upper Colorado River Basin

A Final Report to the Bureau of Reclamation, Lower Colorado Region

June 1, 2012

Connie Woodhouse

With assistance from
Mary Glueck
Brewster Malevich
Holly Faulstich

University of Arizona,
School of Geography and Development,
Tucson, AZ

Table of Contents

1. Introduction

1.1. Overview

This study addresses the nature and potential causes of drought in the upper Colorado River basin (UCRB). Upper basin headwaters yield the majority of total Colorado River flow, and understanding drought and its causes in this region is of critical interest. Between 2000 and 2010, all but two years of annual streamflow at Lees Ferry have been below average, with the lowest value (25% of average) occurring in 2002. The flows have been above average in 2005 and 2008, but just barely so, at 113% and 108% of average, respectively (pers. comm. R. Callejo, 8/30/10). The 10-year period, 2000-2009 has been the driest in the natural flow record for Lees Ferry going back to 1906, which has brought drought to the forefront as a topic of concern. Since this analysis, 2011 has had above average flows, and 2012 is projected to be below average again.

Causes of drought in the UCRB have been linked to El Niño/Southern Oscillation (ENSO), but studies have failed to find a consistent relationship between runoff and ENSO events in the upper basin. There is some there is evidence for responses within the basis, with opposing responses to ENSO in the southern (San Juan River) and northern (upper Green River) portions of the basin (Cayan and Webb 1992, Hidalgo and Dracup 2003, Woodhouse et al. 2006). Overall, the upper basin appears to be transitional with respect to the impacts of ENSO, at least over the period of the gage record (e.g., Woodhouse et al. 2006, Wise 2010). A detailed analysis of how other ocean/atmospheric features impact the basin has not yet been performed, although continental-scale analysis indicates the basin is within a region in which cool season drought is associated with decadal and multidecadal-scale North Pacific/North Atlantic variability (e.g., Enfield et al. 2001, Cayan et al. 1998, McCabe et al. 2004, Moe et al. 2008).

This descriptive report documents the characteristics of upper Colorado River basin drought, the circulation patterns that accompany these droughts, and their possible causal mechanisms on an individual drought event basis. This catalogue of droughts provides evidence for a range of drought characteristics and accompanying atmosphere/ocean circulation features, and a potential baseline for evaluating future droughts.

1.2. Analysis Approach and Data

This report addresses drought and its causes by first identifying a set of six droughts in the UCRB, and examining sub-basin gage records to evaluate the spatial and temporal characteristics of each event. The sequence of flows by year, and the seasonal precipitation and temperature anomalies for the entire basin above Lees Ferry, as well as the sub-basins, are examined. To investigate possible causal mechanism, the circulation patterns accompanying drought conditions are assessed by examining global patterns of pressure (500mb geopotential heights) and sea surface temperatures (SSTs). In addition, a set of circulation indices that reflect tropical and extratropical conditions is compiled in order to get a sense for the state of global oceans and atmosphere during these droughts.

For streamflow, the 1906-2008 natural flow data were used, generated by Reclamation, for nine upper basin tributary gages including: Green R./Green River WY, Green R./Green River UT, Yampa R., Colorado R./Cisco, Gunnison R./Crystal, Gunnison R./Grand Junction, Dolores R., San Juan R./Navajo, and San Juan R./Bluff, as well as for the Colorado at Lees Ferry. For the Lees Ferry gage, we have added the years 2009-2010 as the natural flows became available.

Monthly climate data (total precipitation and average temperature, inches and degrees F) from the gridded PRISM data set (Daly et al. 2008) were downloaded for each sub-basin via the WestMap web site (http://www.cefa.dri.edu/Westmap/). Seasonal total precipitation and average temperatures were based on the water year climatology and the seasonality of moisture delivery. The standard four seasons were not used because they split the water year. Instead, a three-season year was used. Winter (October-February) represents the onset of the water year and the heart of the winter. A spring season, March-May, was differentiated from winter because the delivery of moisture may include upslope storms from east of the basin. The warm season (June-September) represents a period largely dominated by convective storms and warmer temperatures. To simplify circulation analyses, we focused on the winter season. While the months of highest precipitation tend to be March and/or April in most of the sub-basins (Figure 1), the link between seasonal precipitation totals and respective sub-basin water year flow are highest for winter in all sub-basins (Figure 2). The spring season can be very important in certain years, and when winter conditions do not appear to explain drought conditions for a given year, we have also examined the spring conditions.

Seasonal composite maps for the six droughts were also generated from PRISM data using the Westmap mapping tool, with a baseline of 1906-2006 (the original study period at the onset of this project). Occasionally, to show US-wide patterns of precipitation for characterizing larger patterns of drought, US Divisional climate data were used, in the form of standardized precipitation anomalies based on 1895-2000. The slightly variable baselines were not intentional but a function of the flexibility of the mapping tools for the various datasets.

Sea surface temperatures (Smith et al. 2007) and 500mb geopotential height data and images (NCEP/NCAR Reanalysis Dataset, Kalnay 1996) were obtained from the NOAA/ESRL Physical Sciences Division (Boulder, Colorado) web site at http://www.esrl.noaa.gov/psd/. The 500mb data start in 1948, and in these analyses, anomalies are based on the 1981-2010 period. The extended SST data start in 1854, and the same baseline, 1981-2010, was used for consistency.

Circulation indices that describe conditions in the North Pacific (Aleutian Low Index, North Pacific Index, and Pacific North American Index), the equatorial Pacific/ENSO region (Nino 3.4, Pacific Decadal Oscillation –and N. Pacific also), and the northern hemisphere high latitudes (Arctic Oscillation and the Northern Atlantic Oscillation) were also used for this analysis (Table 1). The Atlantic Multidecadal Oscillation (AMO) was considered, but it since only represents three phases during the timespan of these UCRB droughts (with two droughts bridging phase changes), it is mostly included for comparison purposes. We examined indices for the same three seasons generated from the climate data, but focused on the index values for October-February, except for the case of the Aleutian Low Index, which was only available as an annual average). For ease of comparison, we smoothed all index time series, except AMO (which is in either positive or negative), with a three-year running average. Appendix A includes more detailed information on the relationships between most of these circulation indices, global patterns of SST and 500mb geopotential heights, and US precipitation patterns (Divisional data), by season.

It is important to note that correlation maps represent average conditions, and that associations between ENSO, for example, and US precipitation for a given year or set of years can vary from this average. period. The 30-year climatology normal period is used for these maps, but in two cases, maps for two different time periods are shown to illustrate range of variability in spatial patterns. The differences in correlation patterns may due to the decadal scale variability imbedded in some of these circulation features (e.g., Pacific Decadal Oscillation, precipitation patterns show for two phases, Figure A4) or may be due to other factors (including random variability, e.g., Figure A13). These maps, as well as the time series in Figure 5 also show that there are relationships between a number of these indices. In particular the, signature of ENSO in the equatorial Pacific sea surface temperatures is evident in the North Pacific and tropical Pacific indices, indicating the relationship between circulation in this region, primarily in winter and spring. The two North Pacific indices, the Aleutian Low (ALI) and the North Pacific Index (NPI), measure different features, but the time series are essentially mirror images of each other (Figure 5). Both the Artic Oscillation (AO) and the Northern Atlantic Oscillation (NAO) are shown. These are highly correlated with each other, but the correlation patterns indicate the AO is much more relevant for western North America. The AO is much shorter than the NAO; thus both are shown.

The objective of the discussion of the droughts in the context of circulation patterns and indices is not to provide a detailed analysis of the possible causal mechanism over the evolution of the drought but to summarize and highlight the main features that seem to characterize each drought. In all cases, there is no single driver of drought conditions, but I have attempted to describe some conditions that may have been important.

1.3. Definition of drought

Drought identification was based on the natural flow record for Lees Ferry, 1906-2010 (Russ Callejo, personal communication). A drought was defined as a period of consecutively below-average years broken by less than two above-average flow years at Lees Ferry (based on the 1906-2006 mean flow). Initial analyses were based on the years 1906-2006, but 2007-2010 were added as the natural flow estimates became available. Seven droughts were initially identified: 1931-40, 1943-46, 1950-56, 1959-69, 1972-77, 1988-96, and 2000-10. After evaluating these periods, we decide to drop the 1943-46 drought because of its mildness and lack of impact on the Colorado River system.

2. Comparison of All Drought Periods

Table 2 shows the time span of the six droughts, their duration, the number of single years with above-average flow within the drought, cumulative deficits, and average annual deficits. Plots showing the sequence of flows during these droughts are shown in Figure 3. The distribution of below-average flows over the years of each drought across the sub-basins is shown in Figure 4.

A comparison of the six droughts indicates a range of characteristics (Table 2, Figure 3). The longest drought occurred during the period 1959-1969, but as the current drought unfolds, as of 2010, it now matched the length of the 1960s drought. The 1960s drought was broken by two non-drought years, as has the current drought. The longest sequence of unbroken drought is five consecutive years, which occurred during the 1930s, 1980-90s, and current droughts. The largest cumulative deficit has occurred over the current drought (based on 2000-2010), at over 32 MAF

or nearly 3 MAF annually. The second largest deficit occurred during the 1959-1969 period of drought, with a total deficit of 26.4 MAF. The second largest average annual deficit of about 2.5 MAF occurred during the both the 1950s and 1930s droughts. The sequences of drought years show a large range of variability, with some events displaying persistent drought at the onset, like the 1980-90s and the current droughts, while others experience intermittently dry years before plunging into more sustained drought conditions (e.g., 1930s, 1950s). In some cases, severe drought is alleviated by several well-timed above-average flow years (e.g., 1960s, current drought).

The distribution of drought conditions across the upper basin indicates a large degree of spatial homogeneity (Figure 4). Drought years and breaks are often widespread throughout much of the basin, but most remarkably so during the current drought. Regional differences are apparent in the 1950s and 1970s droughts, when the Green River basin experienced a later onset of drought conditions. More spatial variability of drought coverage is evident among basins during the 1930s and 1960s, perhaps because of their length. In both cases, the San Juan River basin (upper in particular) had a relatively greater number of breaks during these periods of drought.

An examination of the circulation indices and their behavior during these six periods of drought reveals a picture of variable ocean/atmosphere conditions (Figure 5). The three North Pacific (Aleutian Low, North Pacific, and PNA) indices vary in a coherent way as expected, but indicate a mixture of positive and negative conditions over any given drought. This is also the case for the tropical Pacific (Nino 3.4 and PDO) and northern high latitude (NAO, AO) indices, as well as the Atlantic multidecadal index.

In summary, this initial assessment indicates no clear picture of a condition or set of conditions that are common to these droughts. Each drought appears to have different characteristics, and is accompanied by a variety of ocean/atmosphere conditions. This necessitates a more detailed look at each of the six droughts to see if it is possible to discern any commonalties among them or among a subset of the droughts.

3. Catalogue of Droughts

3.1. 1930s Dust Bowl Drought

While the geographic heart of the Dust Bowl Drought was in the central Great Plains, the upper Colorado River basin did feel the effects of this drought. The single year, 1934, stands out as the year with the most widespread drought conditions across the entire US, back to at least 1700 (Cook et al. 1999). This drought extended from 1931-1940 in the upper Colorado River basin, broken by two non-drought years, 1932 and 1938 (Figure 6). The most severe drought years were 1931 and 1934, whereas flows in 1936 and 1937 were just below average at Lees Ferry. Across the upper basin, flow conditions were fairly homogeneous, with most sub-basins also experiencing a break in drought conditions in 1936, as well as in 1932 and 1938. The Dolores and San Juan basins had a longer break, with non-drought conditions from 1935/36 to 1938 (Figure 4).

Seasonal precipitation deficits were most consistent, especially for winter, in the White/Yampa, Colorado headwaters, and Gunnison basins (Figure 7). The precipitation deficits in the Green River basin diminished after 1935 for at least some seasons (summer and to some extent, spring).

In the San Juan basin, winter precipitation was below average for all years except 1932 and 1937. Temperatures across the basin were mixed, but were above average for at least one season every year (again, except for 1932). In particular, 1934 and 1938 stand out for their warmth in all seasons and across all sub-basins. In contrast, 1933 is notable for cold temperatures in winter and spring across the UCRB. Spatially, the 1930s winter season had the most complete drought coverage (although absent in the upper Green River basin). Summers were relatively wet in the middle and southern part of the UCRB, while in spring, drought conditions were focused in the lower half of the headwaters basin and in the Gunnison and Dolores basins (Figure 8).

Composite maps of global patterns of seasonal sea surface temperatures (SSTs) suggest generally cool conditions in the equatorial Pacific and warm conditions in the North Atlantic for all seasons from 1931-1940 (Figure 9). In spite of cool equatorial Pacific SSTs, this pattern is not indicative of cool ENSO (see Appendix A). An inspection of winter precipitation anomalies across the US for strongest years of drought in the UCRB (1931, 1934, 1940) (Figure 10) and circulation indices (Figure 5), indicates El Niño conditions in 1931 with the UCRB acting like the Pacific Northwest (i.e., dry conditions), a weak La Niña in 1934 (UCRB coinciding with the typical Southwest US drought response to La Niña), and near neutral ENSO conditions in 1940, with a with a strong Aleutian Low in all these years. In 1940, much of the Great Basin and west was wet, and the UCRB reflected drought conditions in the central and eastern U.S. (Figure 10).

Over the course of this drought, ocean/atmosphere patterns were variable (except for the AMO) with Niño 3.4, N. Pacific, and N. Atlantic indices changing signs over the 10-year period (Figure 5). Hoerling et al. (2009) and Cook et al. (2009) suggest the 1930s cannot be explained by SST anomalies, but instead may have been due to random atmospheric variability exacerbated by dry soils, at least with respect to drought conditions in the northern Great Plains. These suggestions coincide with results shown here, which also indicates a mix of ocean/atmosphere conditions over the course of the drought. The variable UCRB response to ENSO during this period of drought is a demonstration of the transitional nature of the basin with respect to ENSO impacts.

3.2. The 1950s drought: a La Niña drought

The 1950s drought is well-known for its impacts in the southwestern US and the southern Great Plains. It is considered the worst 20th century drought in the US Southwest (Fye et al. 2003). The 1950s drought has been used by some Colorado water providers as the worst-case drought for planning. This drought, defined here as 1950-1956, was most severe (lowest flow) from 1954-1956, and broken by just one non-drought year, 1952 (Figure 11). Sub-basin flows were almost uniformly below average except for the Green River basin, which experienced above average flows in the first two years, and in the last year (Green River near Green River WY only) (Figure 4).

Precipitation deficits were also quite consistent across the sub-basins, with most basins experiencing below-average precipitation across most seasons, again, excepting 1952 (Figure 12). Seasons with above-average precipitation tended to be only slightly above average, again except for 1952 when the winter was quite wet in several sub-basins. As in the 1930s, temperatures were mixed. One of the driest years, 1954, was also remarkably warm in all seasons. In general, winter temperatures tended to be above average during the drought years, while the spring seasons tended to be cooler in at least some basins. Spatially, winter drought

impacted the southern part of the UCRB most strongly, while impacts were more uniform over spring and summer (Figure 13).

This drought is perhaps the most "straightforward" drought in the UCRB, in terms of likely causal mechanisms. Composite SST and 500 mb patterns and circulation indices indicate two La Niña events, in 1950-51 and 1955-56 (Figure 14, left). The PDO phase was negative, which has been shown to enhance the impact of La Niña events (Gershunov and Barnett 1998) (Figure 5). The intervening drought years, 1953-1954, were accompanied by high pressure over western North America, a condition which is conducive to widespread drought (Figure 14, lower right). The AMO remained positive through this period of drought.

3.3. The 1960s drought: the "sleeper" drought

Although the severity of the1950s drought is widely acknowledged (e.g., Fye et al. 2003) and has often been used as a worst-case drought for planning, a drought that followed in the 1960s is rarely mentioned. This 11-year drought spanned 1959-1969, but was broken by two well-placed wet years, which is likely the reason its impact was not more significant (Figure 15). Without those two breaks, an extended run of below-average flows would have followed the 1950s drought, broken by wet conditions in just two years, 1957 and 1958.

Over this interval of drought, the lowest flow years were 1959-1961 and 1963-1964. The years 1962 and 1965 brought relief to these intervals of drought, but relatively moderate drought conditions returned in 1966 and lasted for three more years. In the final year (1969), flow was nearly average (Figure 15). Drought conditions were fairly uniform in the flows across the UCRB, but more consistently dry at the Dolores and lower San Juan (Bluff) basin gages, and somewhat less so at the upper Green River and upper San Juan gages (Figure 4).

Precipitation conditions during the 1960s were seasonally variable across the basin. Spring was most consistently dry throughout the period, while winter precipitation was more often in deficit during the first half of this drought (Figure 16). Of the two wet years, only the winter precipitation was above average (in most cases) in 1962, while all seasons were wet in 1965. Temperatures were most notably above or near average in all seasons from 1959-61 and in 1963. After this, springs and summers were much cooler than average across the basin in 1964-1965 and 1968, alleviating drought conditions somewhat, with modestly above-average temperatures in the intervening years. These patterns, when averaged for the years of the drought, indicate that the most widespread drought conditions occurred in spring (Figure 17). Winters were also dry, although conditions were less severe, and the San Juan basin actually showed positive precipitation anomalies for this drought period. Summers had above-average precipitation, except in the San Juan basin.

During the first part of this drought (1959-1964), circulation was characterized by a ridge of high pressure centered over the northwest US coast (Figure 18, left), promoting dry winter conditions across much of the region. The PNA was strongly positive, with enhanced meridional flow. Low pressure over the Aleutian Islands, coincided with a negative North Pacific Index to help set up this strong PNA flow. This pattern broke down in spring 1964-65. There was a brief El Niño event in 1966 (Figure 18, right), during which the UCRB behaved like the Pacific Northwest in the winter (e.g. experienced drought), although drought conditions became west-wide in spring 1966. Circulation indices indicate a switch in conditions after 1966 (Figure 5), with North

Pacific indices and the PNA reversing signs (as does the AMO), which is reflected in the 500 mb geopotential height pattern for 1967-1968 (Figure 19, left; compare with Figure 18, left). ENSO conditions remained relatively neutral. While the western US experienced variable conditions over these two years, the central US and southern Plains are quite dry, along with much of the UCRB in spring (Figure 19, right). High pressure over the central and southeastern states in spring may be partially responsible for these conditions, possibly causing a ridge that pushed the southwesterly jetstream over the UCRB and east.

In summary, winter drought during the beginning of this period of drought was influenced by high pressure imbedded in meridional flow. The second half of the drought seems to have been influenced by a different set of circulation patterns than the first part. Neither ENSO nor AMO appears to be a consistent feature influencing drought.

3.4. The 1970s drought: Short and Severe

By our definition of drought, the 1970s drought extended from 1972-1977 (Figure 20). However, below-average flows in 1972 and 1974 were separated with above-average flows in 1973 and 1975, and even these two dry years were only slightly below average. This sequence of moderately wet and dry years probably helped buffer the system from the impacts of the severe drought years of 1976 and 1977. The single water year, 1977, was the driest value on record for many gages in the UCRB, including the value for 2002. It remains the worst-case scenario for a single year, but because it was preceded by moderate years and the severity was short-lived, its impact on the Colorado River system was more limited than it might have been. Flows across the basin were fairly coherent for the entire drought event, except at the Green River gages, which did not reflect drought conditions until 1976 (upper Green River) or even 1977 (lower Green River) (Figure 4), and the Yampa, to a lesser degree.

Precipitation was near average or moderately below average in spring and summer in the lower Green, Gunnison, and Colorado headwaters basins through 1976 (Figure 21). Winter conditions were average or slightly below over this period of drought, except in 1973, which was wet to very wet in all sub-basins. Across the entire region, spring and especially winter precipitation was quite low in 1977, although all sub-basins experienced nearly average to slightly above-average summer precipitation. Temperatures over this period of drought were most remarkable for their cool anomalies, particularly in 1973-1975. Moderately warm springs occurred across the basin in 1972 and 1974. In the extremely dry year of 1977, summers were warm in all basins, while winter temperatures ranged from near average to moderately warm everywhere except the San Juan basin. Spring temperatures were very close to average almost everywhere in 1977. Taken as a six-year average, the spatial pattern of precipitation shows the springs and summers were drier than average in most sub-basins, but particularly in the central and southern parts of the UCRB. In contrast, winter precipitation over this period was wetter than average in the southern part of the basin (Figure 22). Clearly, with this degree of averaging, the dry winter of 1977 is not evident.

With respect to circulation, most of the drought period (1973 to 1976) was characterized by coherence in the North Pacific indices and the PNA, which suggested a weakened Aleutian low and a reverse PNA pattern (Figure 5). Composite SST and 500 mb geopotential height maps for winter 1972-1976 show a high pressure anomaly slightly south of the Aleutian Islands, low pressure centered over western North America, and a distinctly cool tropical Pacific (especially

in 1976, but beginning to break down by spring), spreading poleward along the west coasts of North and South America (Figure 23, left). This is in sharp contrast with the SST and 500 mb patterns for winter 1977, which show a warm tropical Pacific, strengthened Aleutian low, and high pressure over western North America (Figure 23, right). Along with the tropical Pacific indices, the PDO also switches sign between 1976 and 1977, from a mode that enhances La Niña impacts (negative phase) to one that enhances El Niño (positive phase). The La Niña-enhanced conditions prior to 1977 coincide with low flows in 1972, 1974, 1976, when the UCRB was behaving like the US Southwest (Figure 24, left). This pattern broke down in 1977, when an area of intense drought becomes centered over the Pacific Northwest, as would be associated with El Niño events, but also it extended throughout the western and central US (Figure 24, top right). The widespread drought conditions of the 1977 water year are not characteristic of El Niño, and indeed, SSTs are only weakly warm in the tropical Pacific (Figure 23, right). Instead, drought in 1977 is more likely attributable to a strong Aleutian Low directing the storm track over a high pressure anomaly that extends from northwestern Canada to southern California (Figure 23, right). The PNA index value for the winter of 1977 is the highest on record, an indication of the extreme meridional flow pattern. Throughout the 1970s, the AMO was in its cool phase, and AO was positive over the middle years of this drought period, suggesting a jetstream contraction northward.

3.5. The 1980s-90s drought

The drought of the late 1980s and early 1990s was one of the worst on record for a large portion of California. Although it was one of the longer droughts in the UCRB (1988-1996), it was relatively moderate in terms of cumulative deficits (Table 2). The nine-year drought was broken by two above-average flow years and ended with nearly average conditions in 1996, all of which helped temper conditions in the second half of the drought. The core of the drought consisted of five consecutive years of below-average flows (1988-1992), which is tied with the 1930s and 2000s drought for the longest run of consecutive drought years (Figure 25). This drought was one of the most spatially consistent, with all sub-basins sharing below- and above-average years until 1996, when all but the Dolores and San Juan gages show above-average flows (Figure 4).

The precipitation patterns by season and basin confirmed that the heart of the drought was the first five years, except for the San Juan basin, which showed a more mixed pattern (Figure 26). Seasonally, winter precipitation was most consistently below average. Spring also shows fairly consistent deficits over the first five years, especially in the lower Green, Yampa/White, and Colorado headwaters basins. The non-drought years of 1993 and 1995 are marked by wet springs. Temperatures are very mixed seasonally and spatially for most basins, but warm anomalies are notably more extreme than cool anomalies (except for 1993) (Figure 26). Spring and summer have the greatest positive anomalies, while winter anomalies of either sign tend to be more moderate. The upper Green River basin, in particular, showed consistently above-average temperatures over this period of drought (except for 1993).

When composite maps for seasonal precipitation are examined, winter precipitation anomalies are mixed across the basin. Summer is more consistently dry, while spring shows mostly above-average precipitation for all but the upper San Juan basin (Figure 27). This pattern is likely attributed to the wet springs of 1993 and 1995.

Over the course of the core years of this drought, 1988-1992, tropical Pacific SSTs swing from conditions reflecting El Niño to La Niña and back to El Niño between 1988 and 1992 (Figure 28, left). Precipitation patterns in 1988 and 1992 show dry conditions in the upper part of the UCRB, and a larger pattern of drought indicative of the Pacific Northwest response to El Niño (Figure 29; conditions similar for spring). In two these winters, significant drought extends from central California to the northern Great Plains, dipping into the Great Basin and the northern portions and headwaters of UCRB. In 1989-1991, an extended period of relatively cool SSTs in the tropical Pacific may have helped promote drought (Figure 28). However, widespread winter drought across much of the western US in these years may be more attributable to the 500 mb pattern of pressure, in which an elongate pattern of high pressure from Asia to the Atlantic forced the jet stream north across northern North America. This pattern is supported by a negative PNA pattern and a weakened Aleutian Low, conditions similar to those in the first part of the 1970s drought. Also similar to the 1970s, the AO is positive, with zonal flow tracking in a more poleward direction. The AMO is negative during most of this drought, though it switches phase near end.

3.6. 2000s drought – a global warming drought?

The 2000s drought began in the fall of 1999 (Pielke et al. 2005), extended through 2010 (water year flows in 2011 were on the order of 120% of average, but 2012 will be below average again). The first five years of the drought were the most severe (2000-2004), characterized by one of the lowest flow years on record, 2002 (2nd only to 1977), and one of longest runs of consecutive drought years (shared with 1933-37 and 1988-1992) (Figure 30). After this run of low flow years, the remainder of the drought was broken by two years of slightly above-average flows (2005, 2008). Flows at Lees Ferry from 2006-2010 varied from moderately above to moderately below average. The pattern resembles the 1980s-90s drought to some extent, although the second half of this drought has been more prolonged. In addition, the magnitudes of the flows differ, with cumulative deficits over the 5-yr low flow period being more severe during the 2000s drought (46.8 MAF in 1988-92 versus 54.4 MAF in 2000-05), and the above-average year flows were not a high as the 1980-90s wet years. Flows across the basin were uniformly below average in 2000-2004 (Figure 4). Above-average flows brought some relief in 2005, especially in the Dolores and San Juan gages, and in all but one of the Gunnison gages. Drought returned to all sub-basins except the White/Yampa basin in 2006, but was again below average in all basins in 2007. In 2008, all but the Green River sub-basins, had above average flows.

Precipitation deficits over the first five years of this drought were most consistent in the Gunnison, White/Yampa, and upper Green River watersheds, especially in winter and spring (Figure 31). The lower Green and San Juan watersheds experienced slightly above-average conditions in the winter of 2001. While the winter-spring of 2002 was uniformly the driest year in all basins, the spring of 2003 showed a slight recovery in the Colorado headwaters, likely the result of one upslope storm in March of that year. Precipitation in the second half of this drought period was mixed. The watersheds in the central part of the basin (White/Yampa, Colorado headwaters, Gunnison, and the lower Green to some extent) experienced mostly above-average winter (and sometimes summer) precipitation from 2006-2009, while spring precipitation was mostly below average. The upper Green River basin tended to be drier or near average over this period, and the San Juan was quite mixed.

In general, the precipitation deficits do not stand out compared to those of other periods of drought, but what are anomalous are the temperature departures (Figure 31). Temperatures across nearly all seasons and all basins were consistently above average from 2000-2007. In 2008 and 2010, springs were cool and winters cool or near average. Summer temperatures stand out as being the most consistently above average in all basins throughout the 11-year period.

Spatial patterns of drought over the full drought period show a mix of conditions in winter, with fairly widespread drought in spring and summer (Figure 32). In contrast, the pattern of drought in winter for the first five year shows markedly drier conditions.

The first five years of this drought were initially characterized by cool tropical Pacific SSTs (2000-2002), which then switched to weak El Niño/warm tropical Pacific conditions in 2003-2004 (Figure 33), with indices of North Pacific circulation indicated a strong Aleutian low and meridional flow during this time. The switch in tropical Pacific conditions was accompanied by a corresponding switch in the sign the PDO (negative to positive) (Figure 5). Although cool SSTs characterized the winters of 2000-2002, the western North American pattern of precipitation did not reflect this in 2001, which was relatively wet in the Southwest and dry in the Pacific Northwest (a small center of low pressure on the coast of southern California appears to be responsible for this anomaly). The impact of El Niño conditions in 2003-2004 appear to have been weakened by a jet stream tracking far north (Figure 33, bottom right), agreeing with positive AO values (Figure 5). From 2006 to 2008, circulation indices fluctuated around zero, and composite SST and 500 mb maps for the dry years, 2006-2007 show no distinct patterns, except for a tongue of moderate high pressure extending across the North Pacific and into western North America (Figure 34). Conditions switched again between 2009 and 2010 from a weak to strong Aleutian Low, and from weak La Niña to weak El Niño conditions.

4. Summary of Main Features of Droughts

It is clear that the droughts of the UCRB are widely varied in terms of temporal and spatial characteristics. It is also obvious that a large number of circulation patterns and mechanism, and different sequences of these combine to produce multi-year droughts. In order to seek some clarity regarding common conditions that appear to accompany drought, composite maps of 500 mb and SSTs were generated for eight lowest flow years, that is, those years with flows < 10 MAF at Lees Ferry.

The composite maps indicate a distinctive 500 mb pressure pattern, but a much more variable pattern of SSTs (Figure 35). The 500 mb composite features a relatively strong Aleutian Low, a high pressure anomaly centered just east of the US west coast, and low pressure over northeastern North America. The pattern is reminiscent of the PNA pattern with a slight, but critical shift in the high pressure anomaly over western North America (Figure 36). In the PNA correlation field map, the high is centered over western Canada, a position north and east of that in the drought composite map. In the PNA, low pressure is centered in the southeastern US, while the in drought composite, this low is over northeastern North America. Thus, the Aleutian Low appears to be a common feature, but the position of the high pressure over the western US seems to be the critical feature for drought, and the pressure pattern is more of a wave train centered between 45º - 50ºN than a classic PNA pattern. The position of the Aleutian Low and the high pressure over the coast of western North America would result in a jetstream that is directed north above most of the western US. In addition, the position of the wave train suggests

the jetstream is contract toward the pole, leaving much of the western and central US below its track. Not surprisingly, these extreme low flow years are also severe drought years in other areas (Figure 37). A composite map of standardized precipitation anomalies for US Climate Divisions for these eight years shows widespread and severe drought from California, across the Great Basin, the northern and central Great Plains and most of the eastern US. Areas with above average precipitation are limited to the far Pacific Northwest and the Gulf Coast area from southern Texas to Florida.

The composite map of SSTs features a bulge of cool water off the coast of South American and just south of the equator, with little similarity to the classic ENSO pattern (Figure 35, right). The strongest anomalies are in the far northeastern Pacific with a small areas of cool SSTs south of the Aleutian Islands (perhaps a reflection of the low pressure), and in the southeast Pacific Ocean. The pattern in the North Pacific again, is just slightly reminiscent of the PNA SST pattern (Appendix A). The far northern and northeastern North Atlantic is warm, and the pattern is not similar to any of those of circulation indices.

These results suggest more dynamic atmospheric conditions that influence the polar jetsteam may be more likely to influence drought than the equatorial Pacific SST-driven conditions of ENSO. In addition, this also suggests that a variety of circulation influences could result in drought if they influence the jetstream in such a way as to set up the Aleutian Low and high over western North American in just the right way.

5. Literature Cited

Cayan, D.R., and R.H. Webb, 1992. El Niño/Southern Oscillation and streamflow in the western United States, *in* Diaz, H.F., and Markgraf, V., (editors), El Niño, Historical and paleoclimatic aspects of the Southern Oscillation: Cambridge, England, Cambridge University Press, p. 29-68.

Cook, B., R. Miller, and R. Seager, 2009. Amplification of the North American ‘‘Dust Bowl’’ drought through human-induced land degradation. Proceedings of the National Academy of Sciences 106, 4997-5001, doi:10.1073/pnas.0810200106.

Cook, E. R., D. M. Meko, D. W. Stahle, and M. K. Cleaveland, 1999. Drought reconstructions for the continental United States, Journal of Climate 12, 1145 –1162.

Daly, C., M. Halbleib, J.J. Smith, W.P. Gibson, M.K. Doggett, G.H. Taylor, J. Curtis, and P.A. Pasteris, 2008. Physiographically-sensitive mapping of temperature and precipitation across the conterminous United States. International Journal of Climatology, DOI: 10.1002/joc.1688.

Enfield, D.B., A.M. Mestas-Nunez, and P.J. Trimble, 2001. The Atlantic Multidecadal Oscillation and Its Relation to Rainfall and River Flows in the Continental U.S. Geophysical Research Letters 28, 2077-2080.

Fye, F.K., D.W. Stahle, and E.R. Cook, (2003. Paleoclimatic analogues to 20th century moisture 3regimes across the U.S. Bulletin of the American Meteorological Society 84, 901– 909, doi: 10.1175/BAMS-84-7-901

Gershunov, A. and T.P.Barnett, 1998. Interdecadal modulation of ENSO teleconnections. Bulletin of the American Meteorological Society 79, 2715-2725.

Hidalgo, Hugo G., John A. Dracup, 2003. ENSO and PDO Effects on Hydroclimatic Variations of the Upper Colorado River Basin. Journal of Hydrometeorology 4, 5–23.

Hoerling, M., X. Quan, and J. Eisheid, 2009. Distinct causes for two U.S. droughts. Geophysical Research Letters 36, L19708, doi:10.1029/2009GL039860,

Kalnay E., et al. 1996. The NCEP/NCAR 40-Year Reanalysis Project. Bulletin of the American Meteorological Society 77, 437-471.

McCabe, G.J., M.A. Palecki, and J.L. Betancourt, 2004. Pacific and Atlantic Ocean Influences on Multidecadal Drought Frequency in the United States. Proceedings of the National Academy of Sciences 101, 4136-4141.

Mo, K.C., J-K. E. Schemm, and S-H Yoo, 2009. Influence of ENSO and the Atlantic Multidecadal Oscillation on Drought over the United State. Journal of Climate 23, 5962-5982.

Pielke, R.A., N. Doesken, O. Bliss, T. Green, C. Chaffin, J.D. Salas, C.A. Woodhouse, J.J. Lukas, and K. Wolter. 2005. Drought 2002 in Colorado – An Unprecedented Drought or a Routine Drought? Pure and Applied Geophysics (PAGEOPH) 162, 1455-1479.

Smith, T.M., R.W. Reynolds, T. C. Peterson, and J. Lawrimore, 2007. Improvements to NOAA's Historical Merged Land-Ocean Surface Temperature Analysis (1880-2006). In press. Journal of Climate.

Wise, E.K. 2010. Spatiotemporal variability of the precipitation dipole transition zone in the western United States. Geophysical Research Letters, 37 (L07706), doi:10.1029/2009GL042193.

Woodhouse, C.A., S.T. Gray, and D.M. Meko, 2006. Updated streamflow reconstructions for the Upper Colorado River basin. Water Resources Research, 42, W05415. doi:10.1029/2005WR004455.

Appendix A

Correlation fields for seasonal circulation indices with SSTs, 500mb geopotential heights, and divisional precipitation data.

Correlation period is 1981-2010, expect for precipitation patterns for Nino 3.4 and PDO (2 phases of PDO are shown), and precipitation patterns for AMO (2 phases are also shown).

Indices:

- Nino 3.4
- PDO
- PNA
- NP
- NAO
- AO
- AMO (precipitation patterns only)

Note: significance levels are not provided. These are for qualitative assessment only.

Data and image provided by the NOAA/ESRL Physical Sciences Division, Boulder Colorado from their Web site at http://www.esrl.noaa.gov/psd/

Seasonal Correlations with Nino3.4

Sea Surface Temperatures

500mb Geopotential Height

Oct-Feb

Mar-May

Jun-Sep

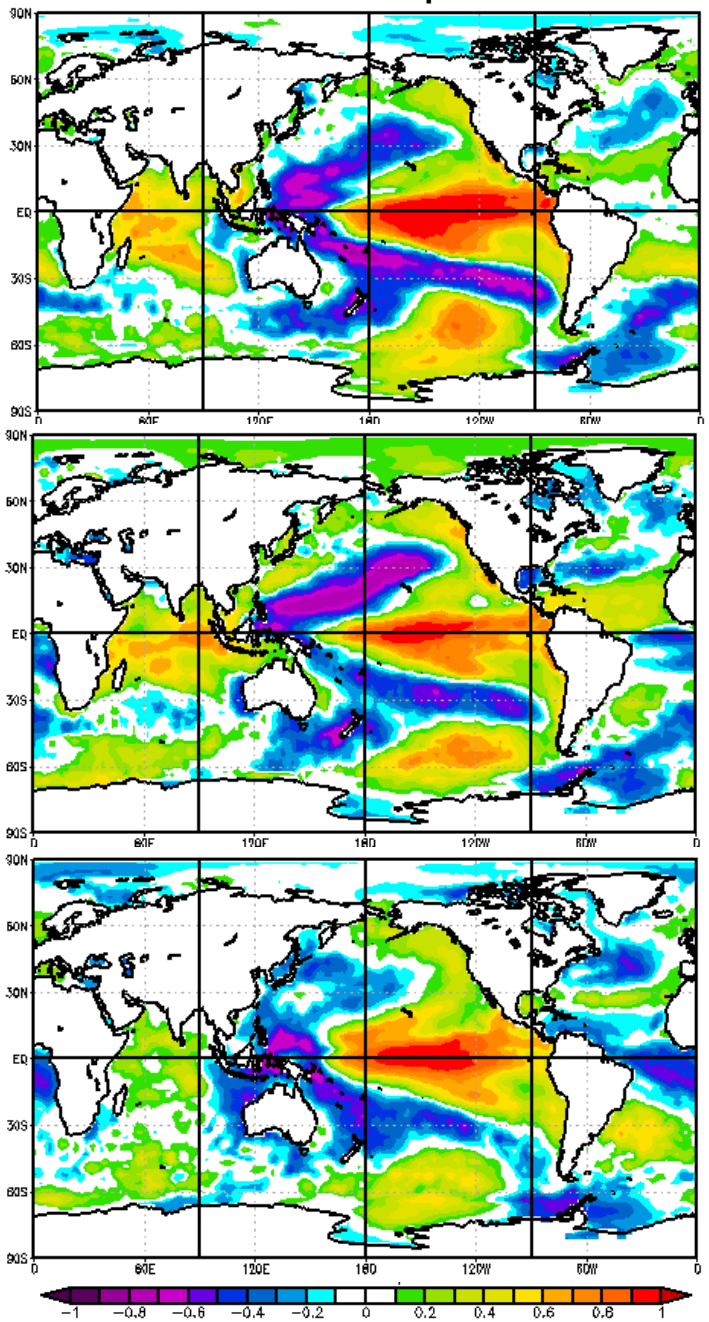

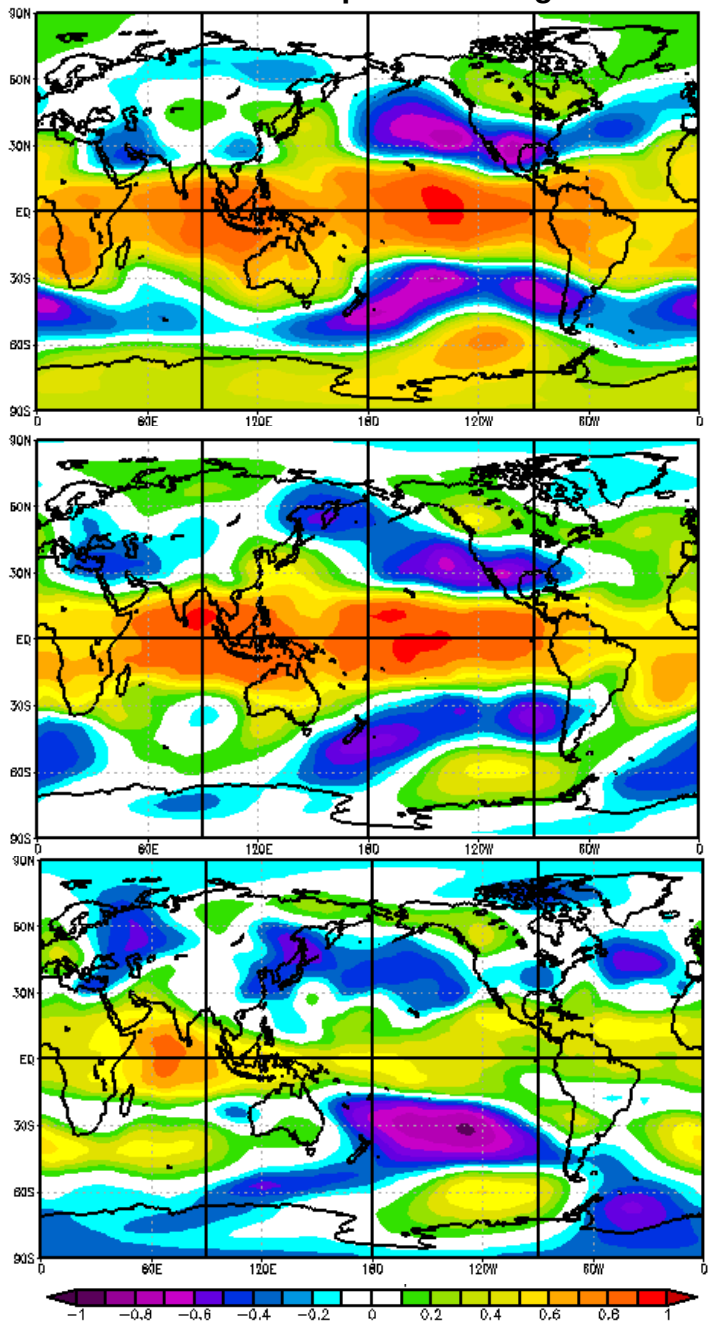

1981-2010

A1

Divisional Precipitation Correlations with Nino3.4

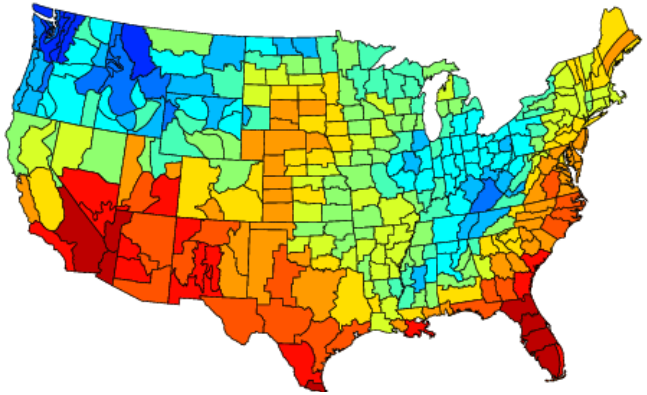

Oct-Feb

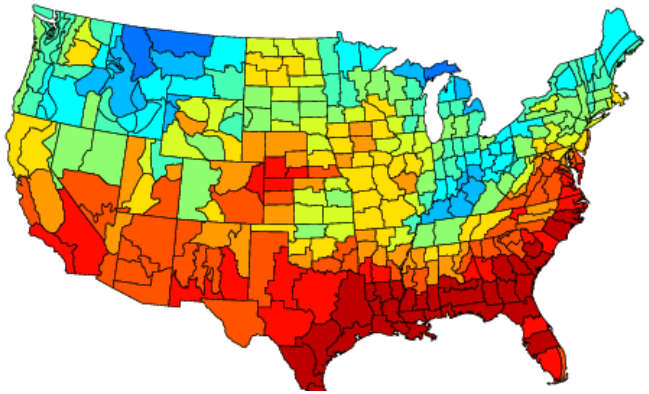

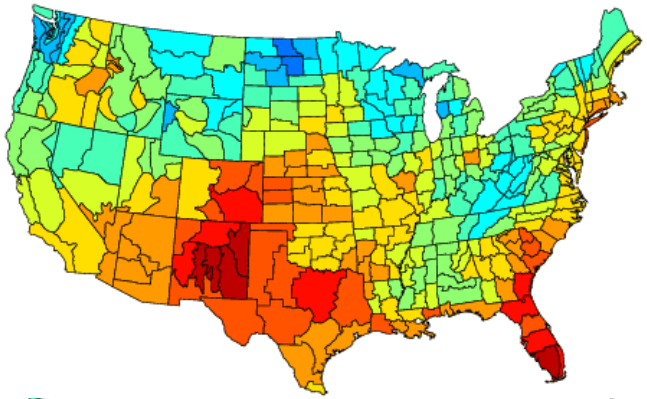

Mar-May

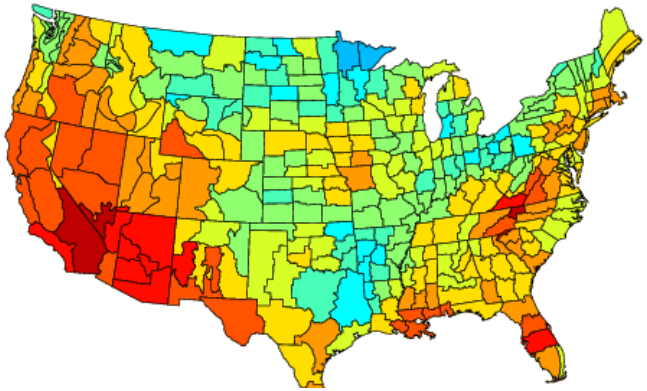

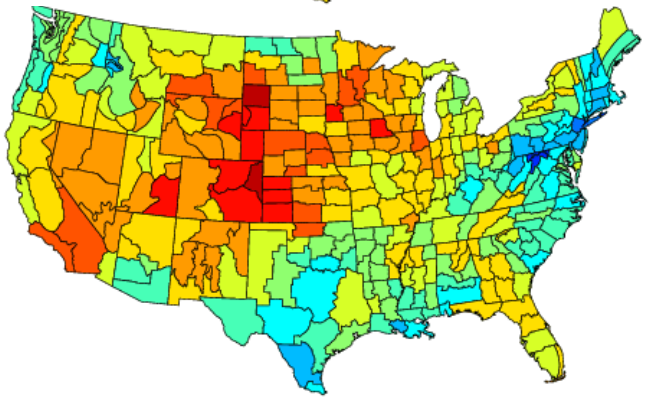

Jun-Sep

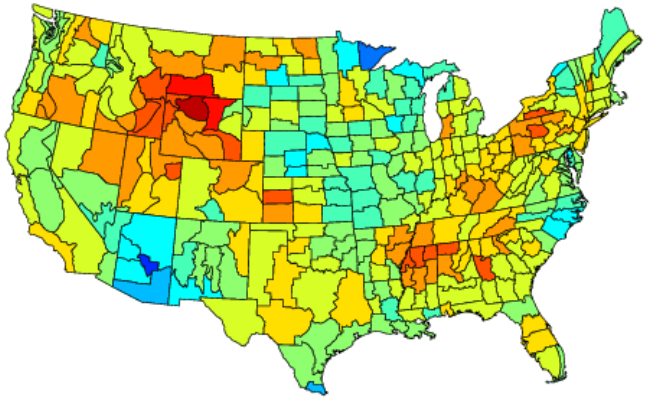

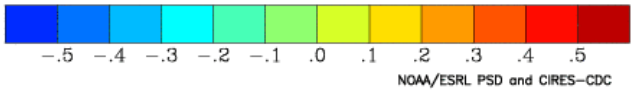

A2

1948-1980

1981-2010

Seasonal Correlations with PDO

Sea Surface Temperatures

500mb Geopotential Height

Oct-Feb

Mar-May

Jun-Sep

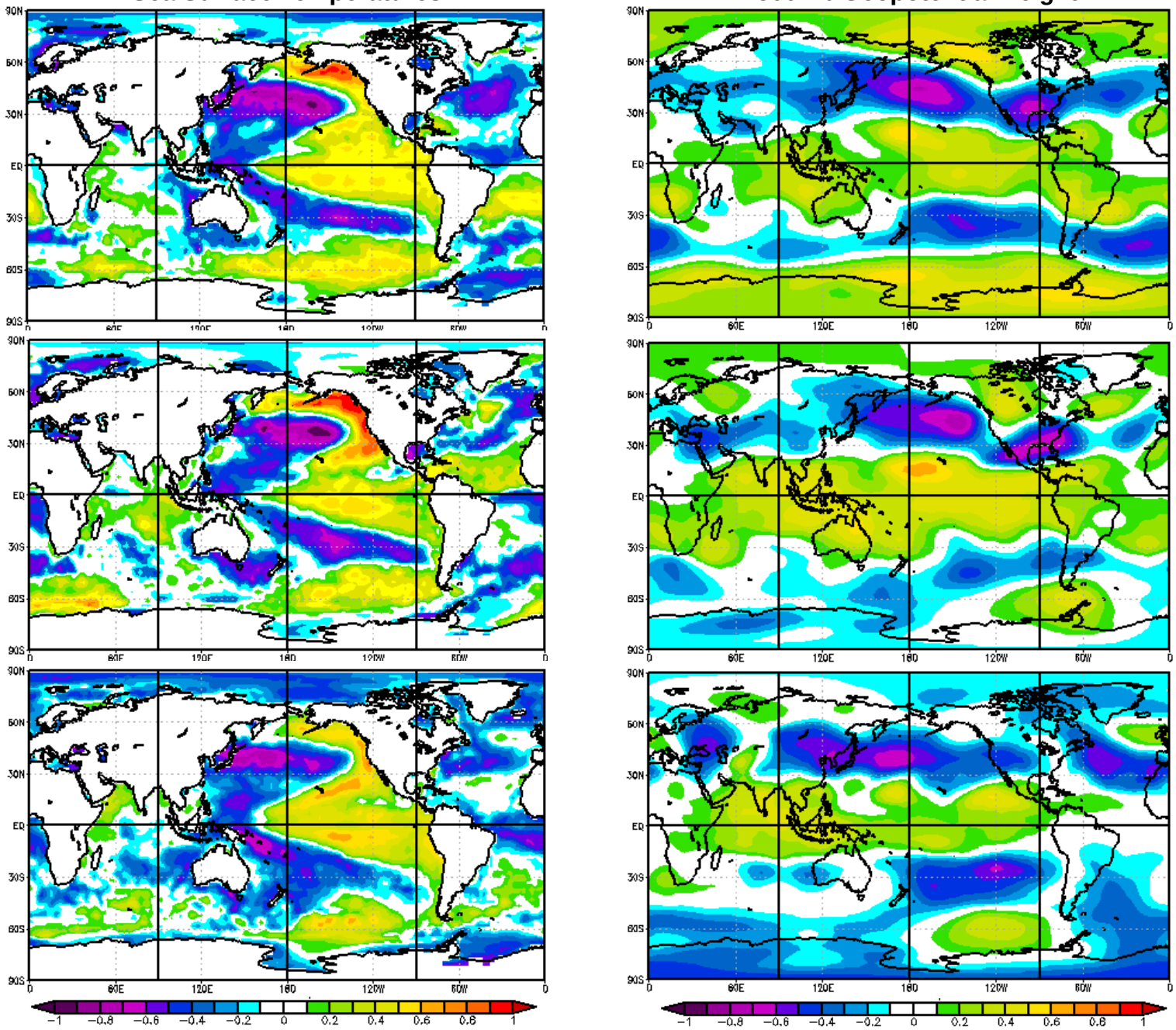

A3

1981-2010

Divisional Precipitation Correlations with PDO

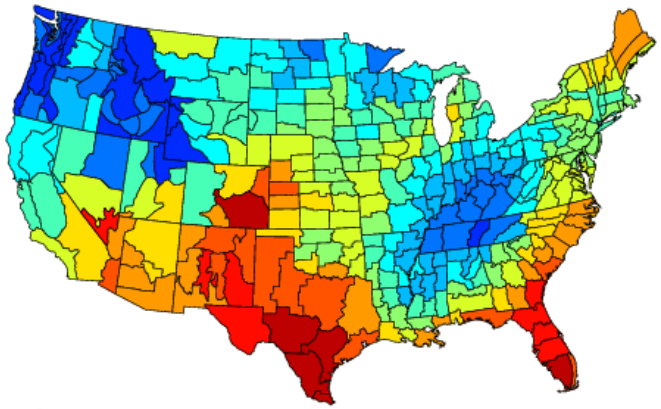

Oct-Feb

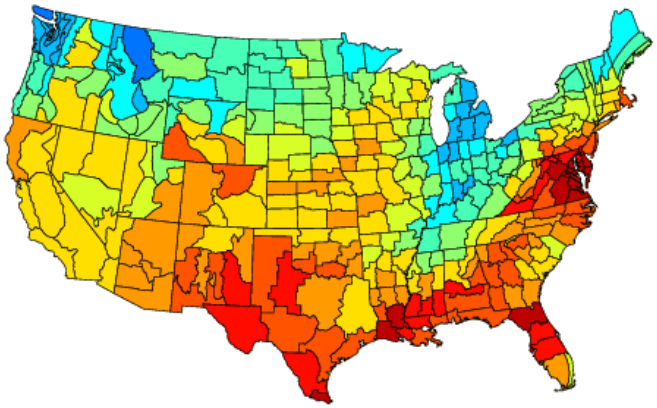

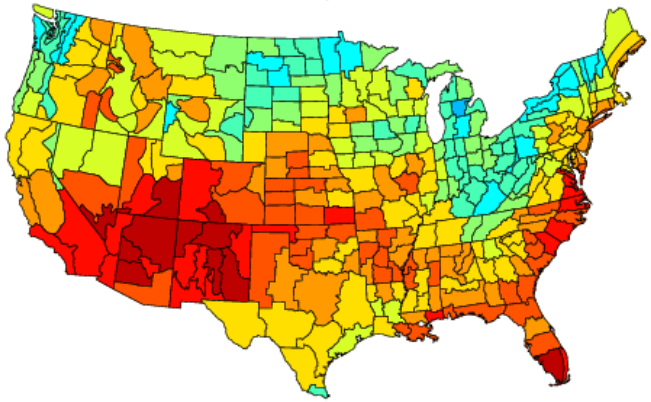

Mar-May

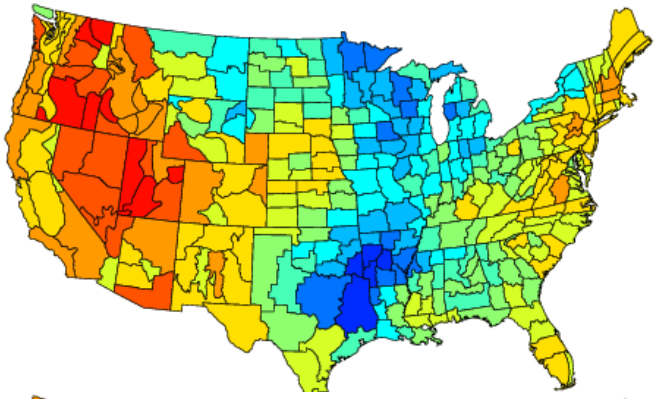

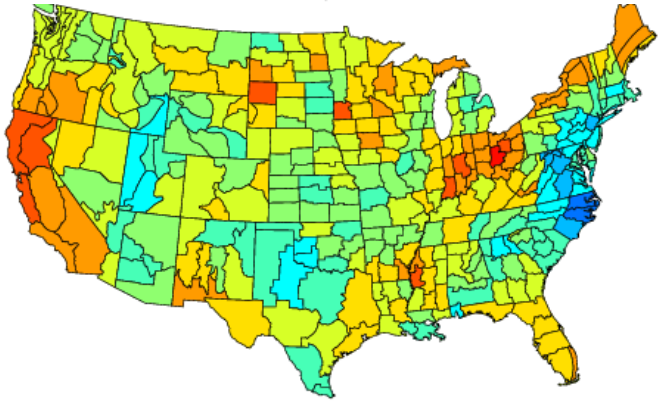

Jun-Sep

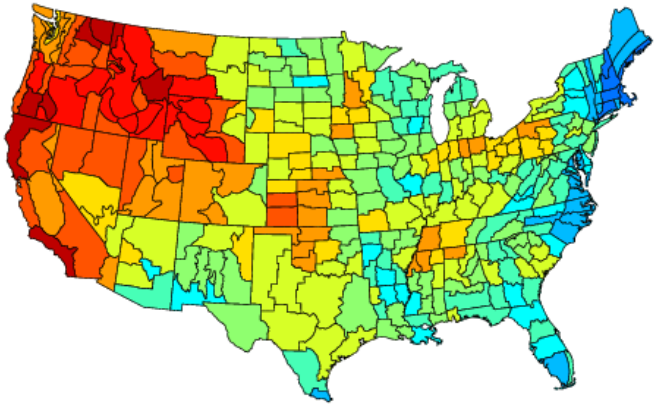

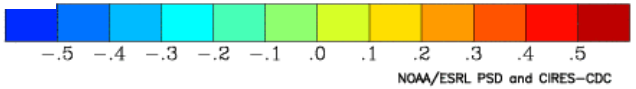

A4

1948-1980

1981-2010

Seasonal Correlations with PNA

Sea Surface Temperatures

500mb Geopotential Height

Oct-Feb

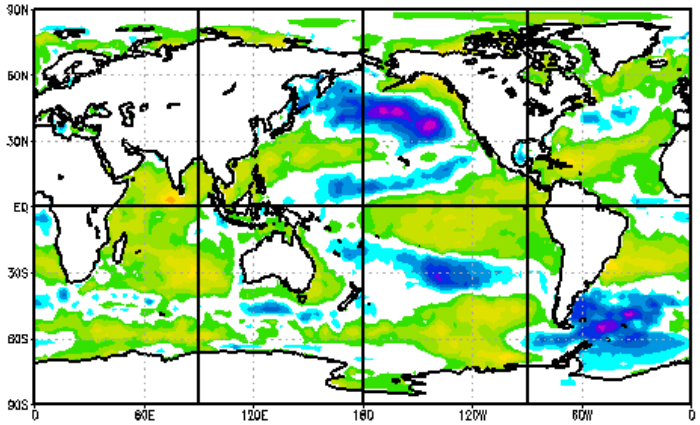

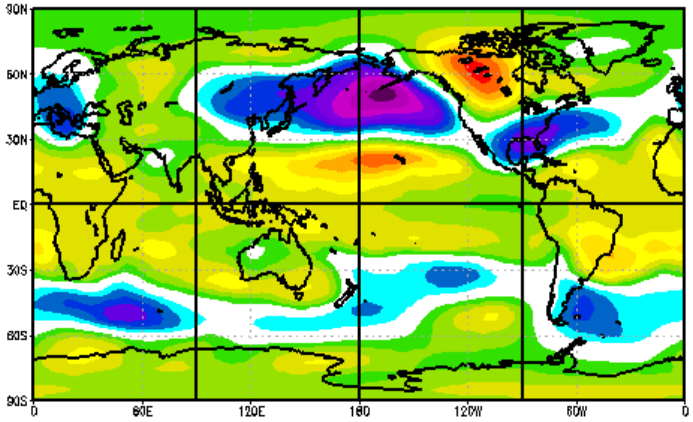

Mar-May

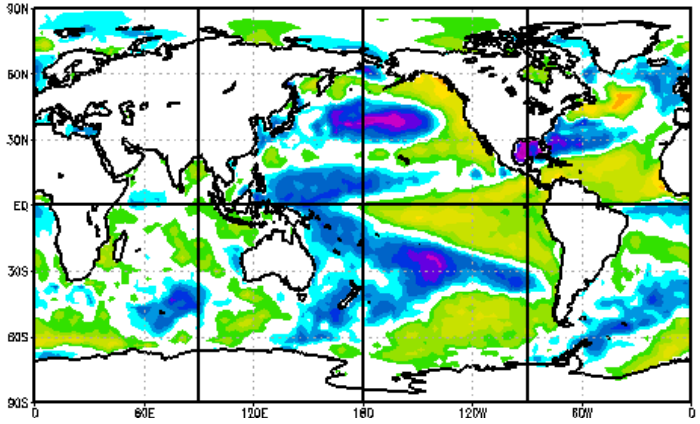

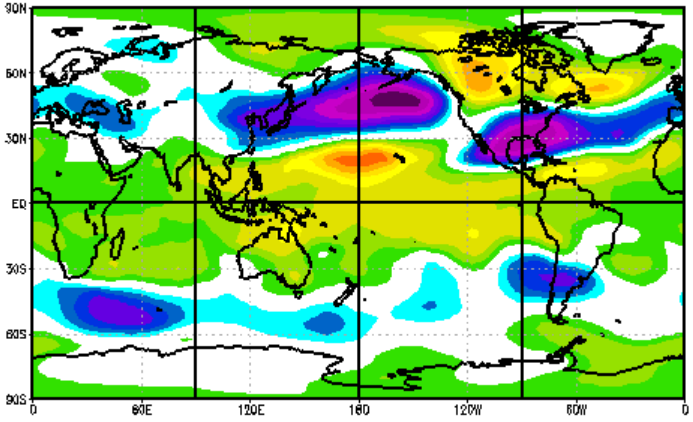

Jun-Sep

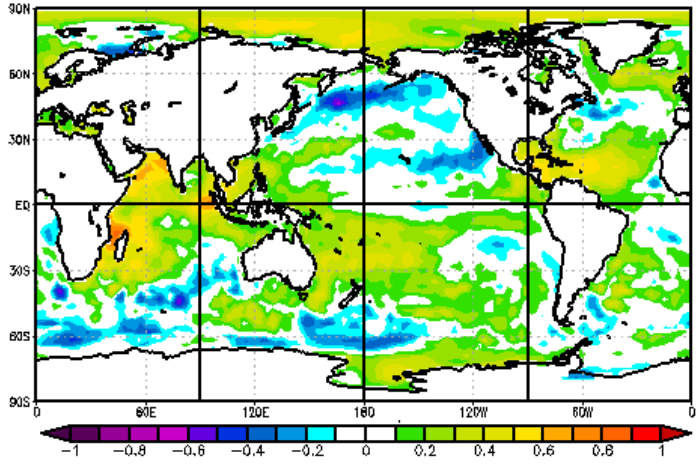

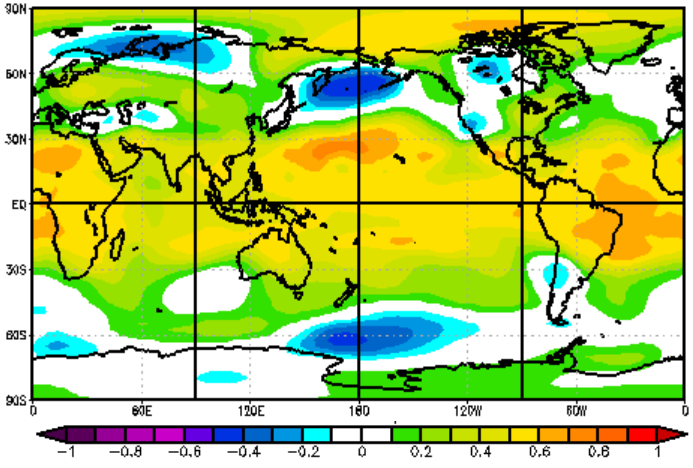

1981-2010

Divisional Precipitation Correlations with PNA

Oct-Feb

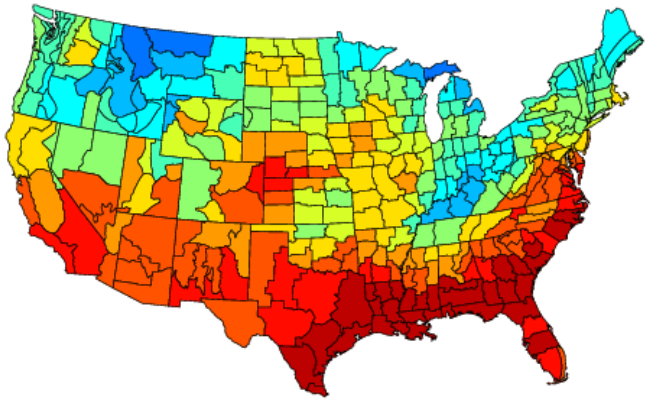

Mar-May

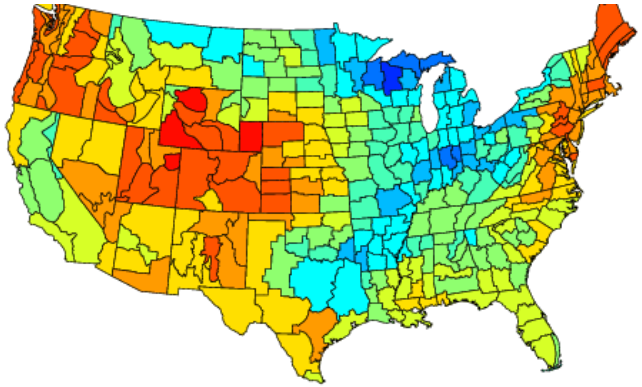

Jun-Sep

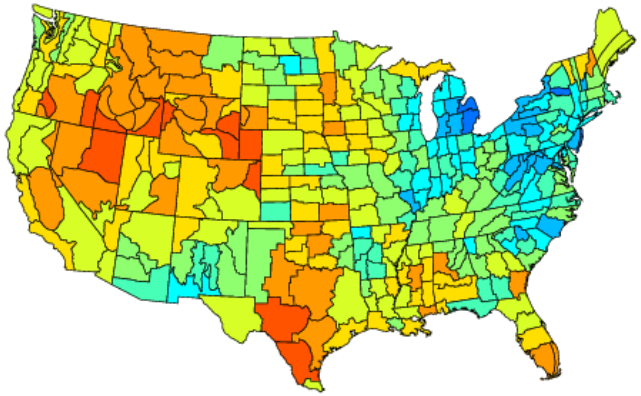

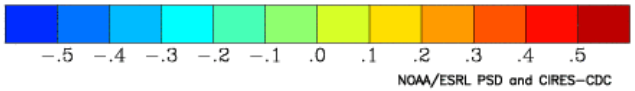

1981-2010

Seasonal Correlations with NP

Sea Surface Temperatures

500mb Geopotential Height

Oct-Feb

Mar-May

Jun-Sep

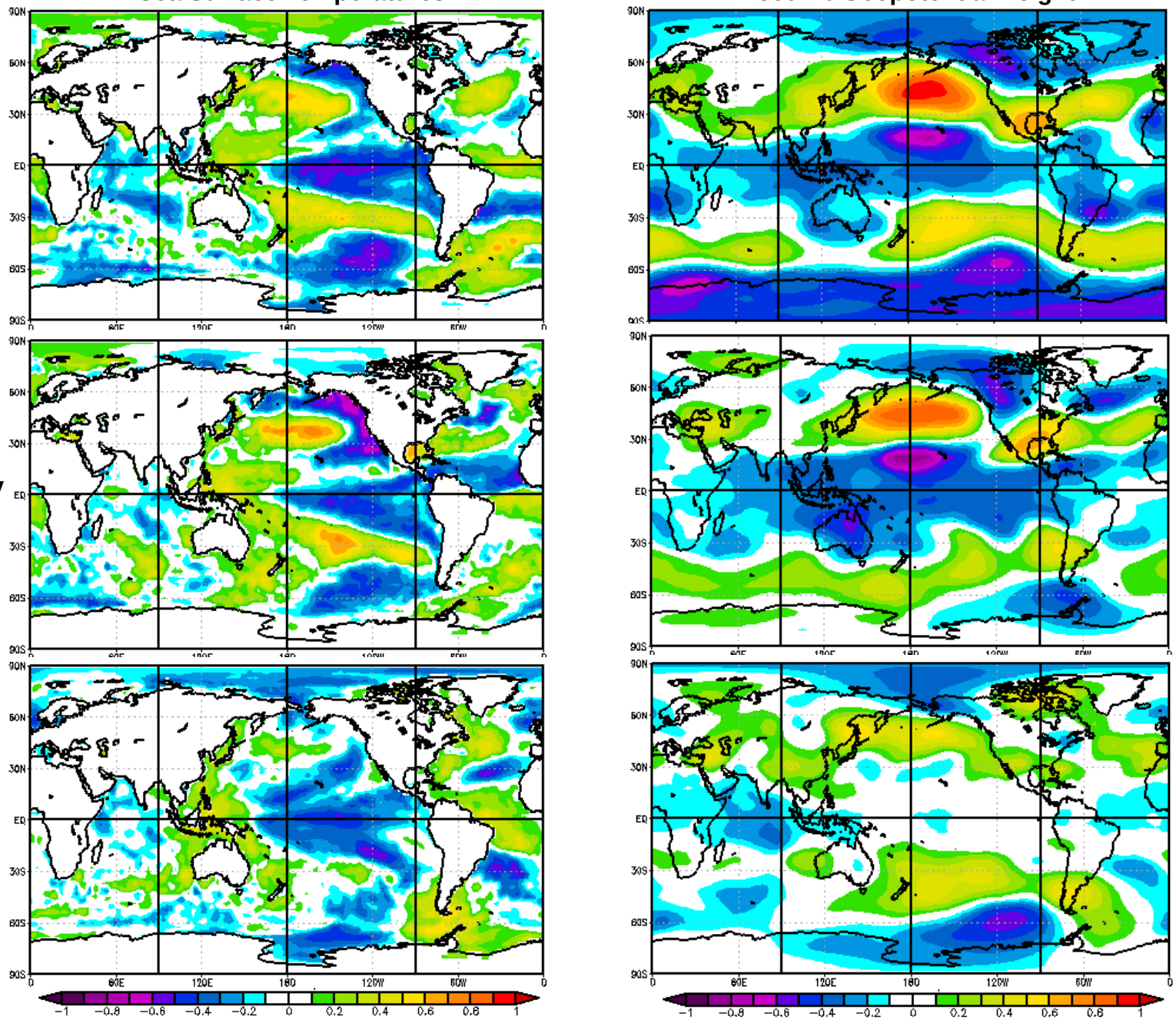

1981-2010

Divisional Precipitation Correlations with NP

Oct-Feb

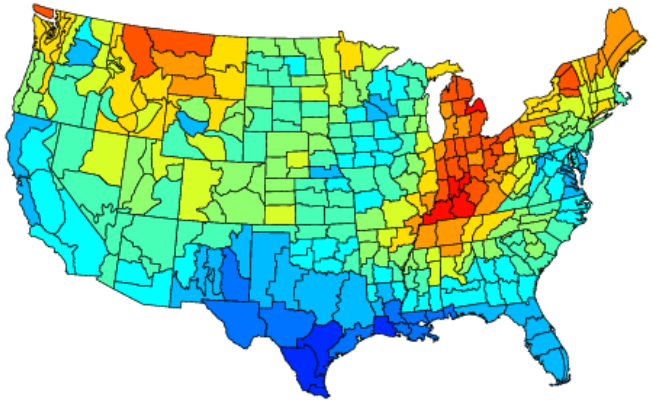

Mar-May

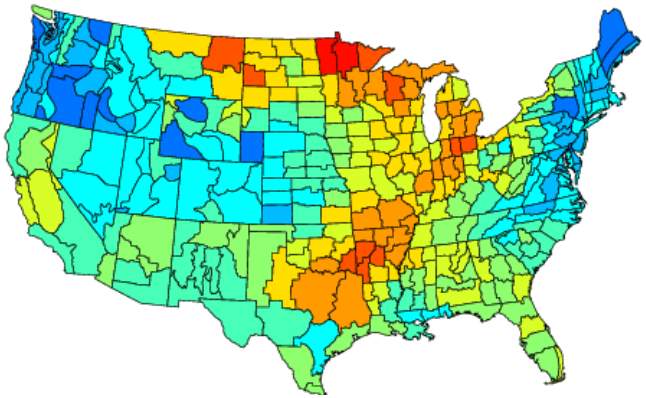

Jun-Sep

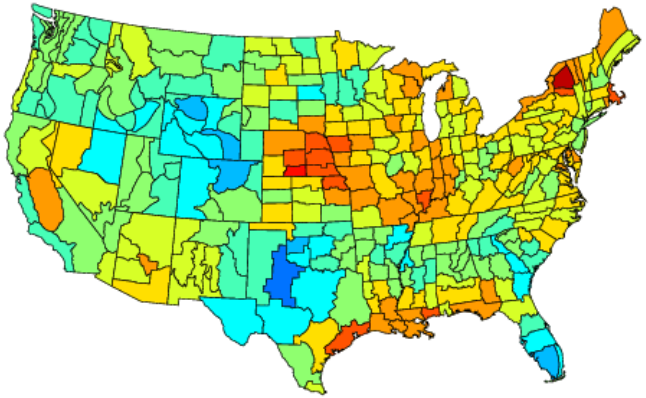

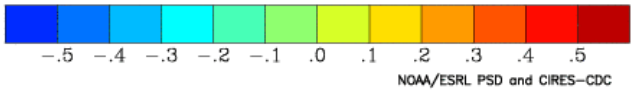

1981-2010

Seasonal Correlations with NAO

Sea Surface Temperatures

500mb Geopotential Height

Oct-Feb

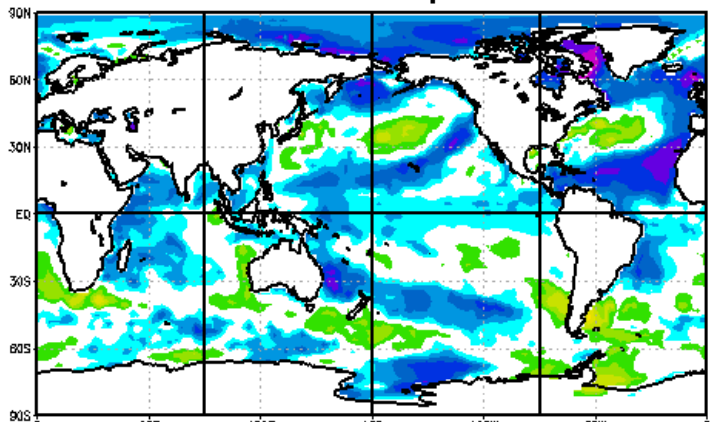

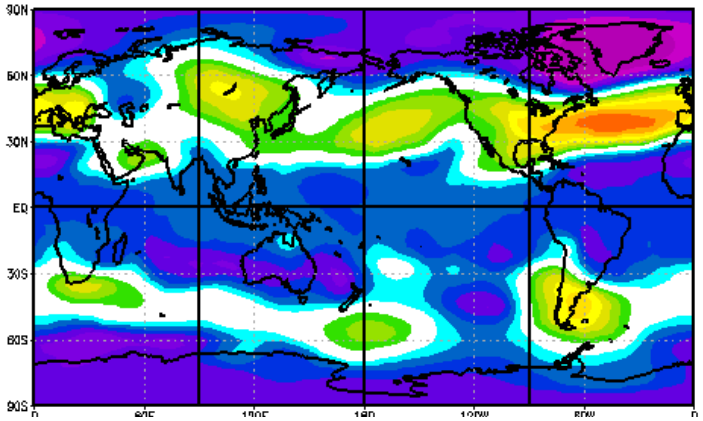

Mar-May

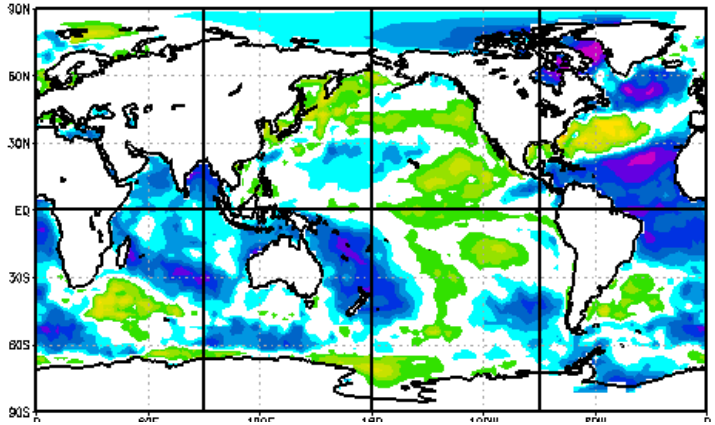

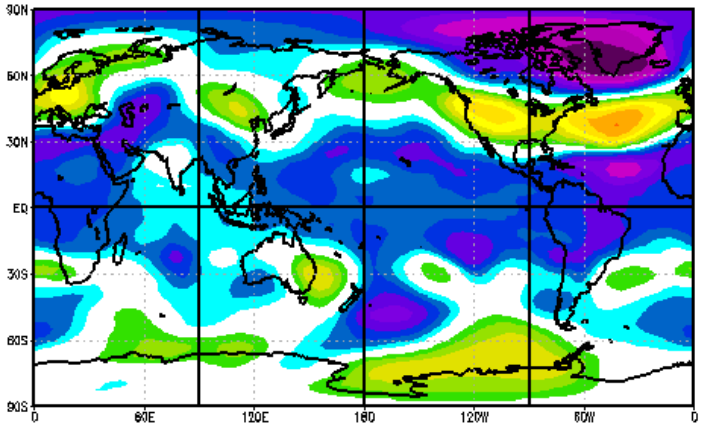

Jun-Sep

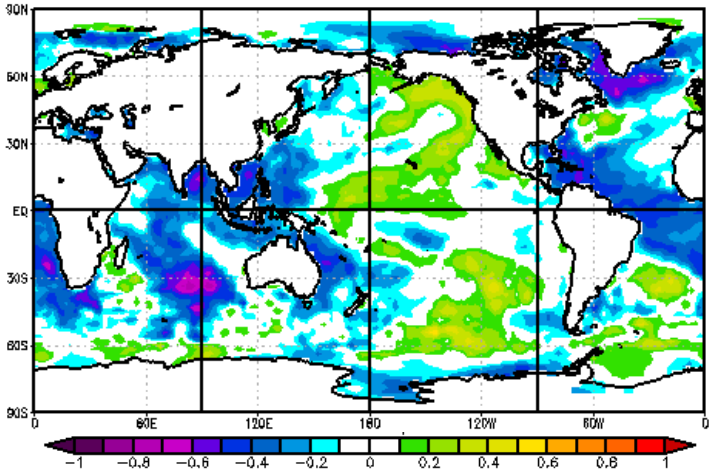

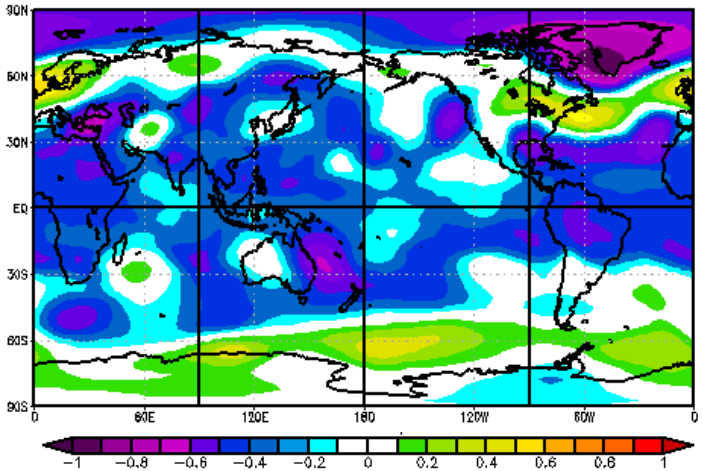

1981-2010

Divisional Precipitation Correlations with NAO

Oct-Feb

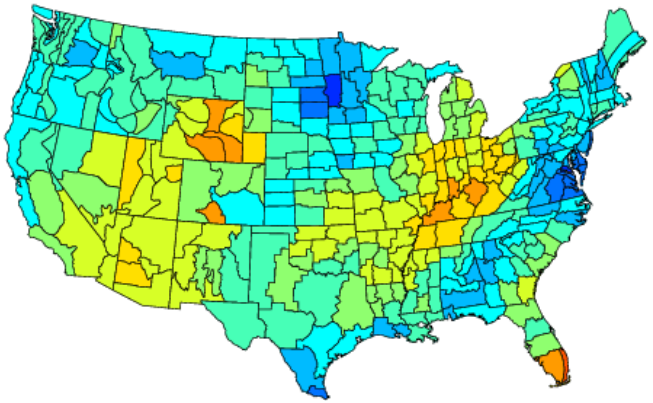

Mar-May

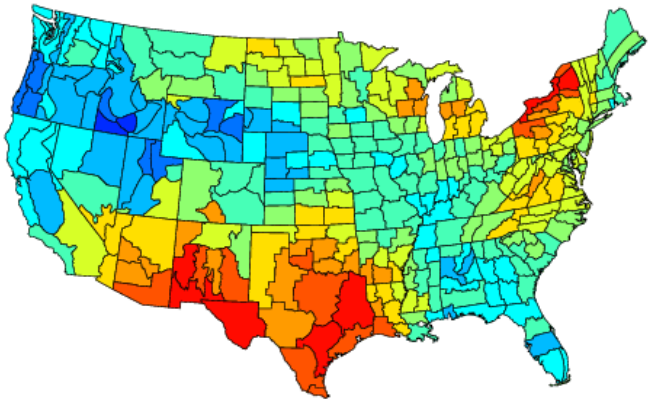

Jun-Sep

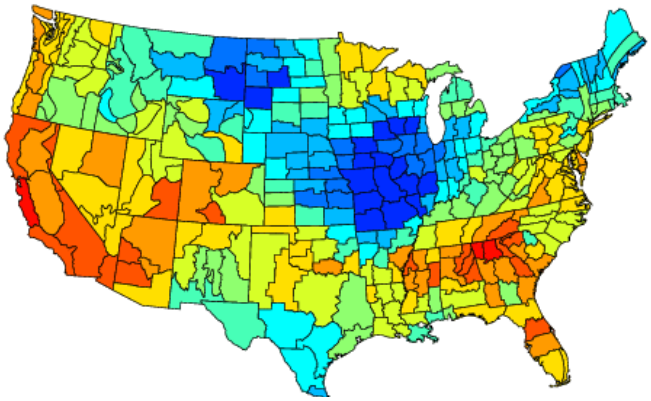

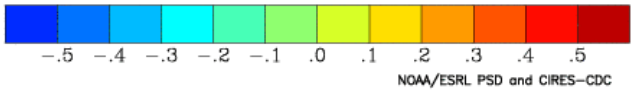

1981-2010

Seasonal Correlations with AO

Sea Surface Temperatures

500mb Geopotential Height

Oct-Feb

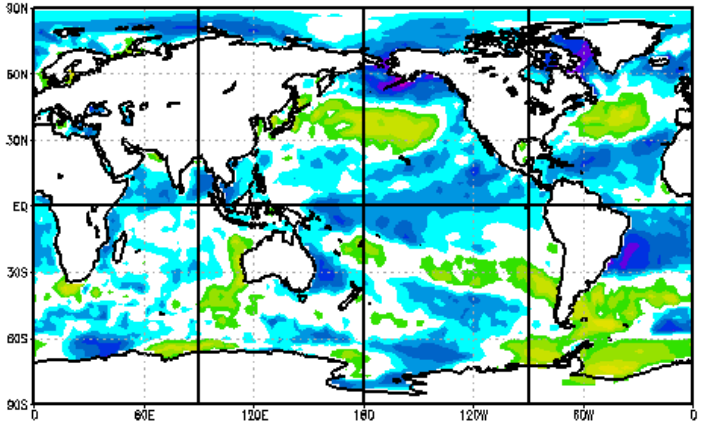

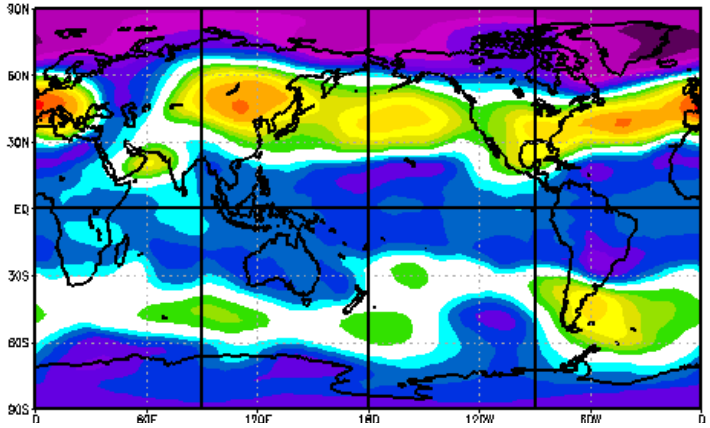

Mar-May

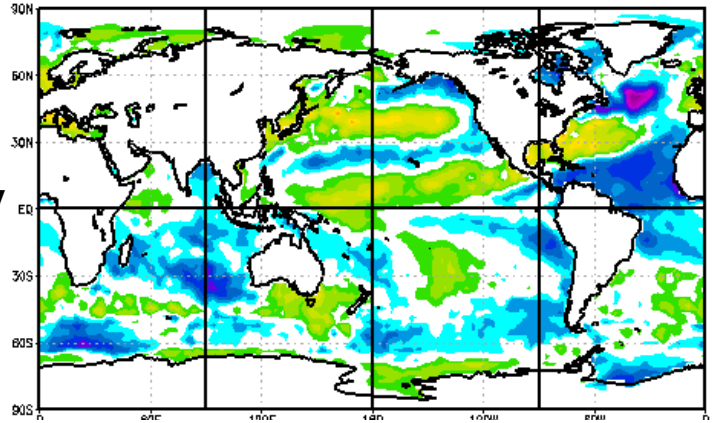

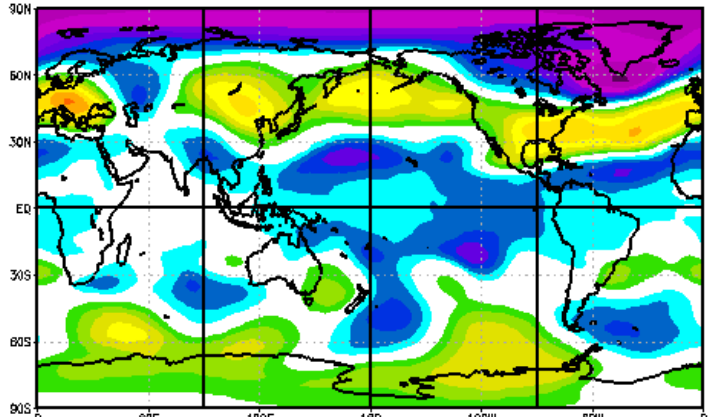

Jun-Sep

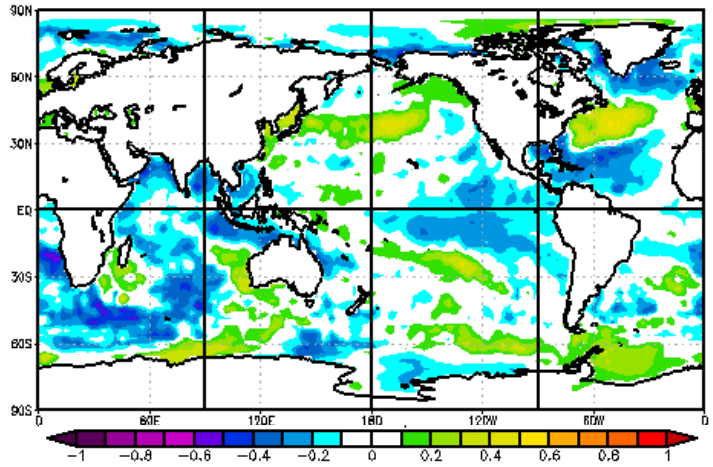

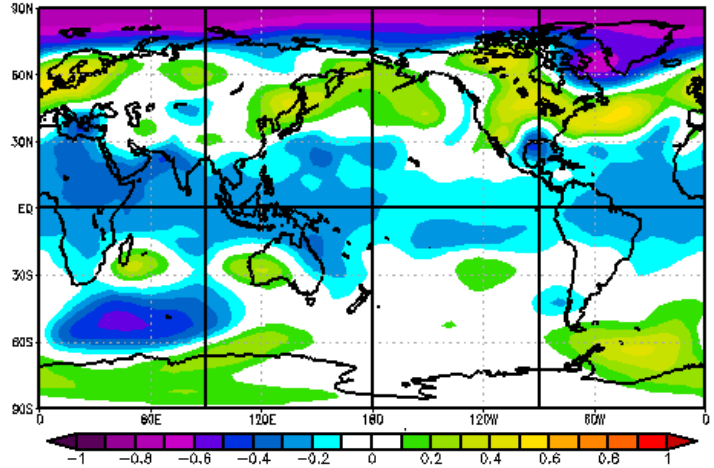

1981-2010

A11

Divisional Precipitation Correlations with AO

Oct-Feb

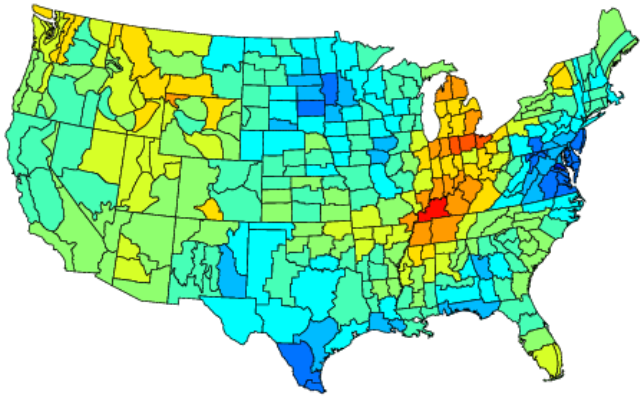

Mar-May

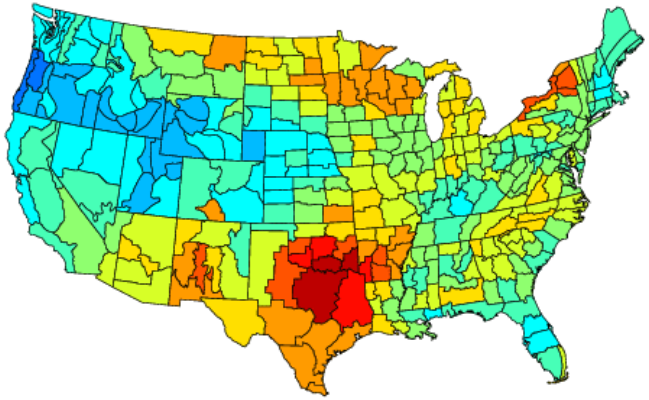

Jun-Sep

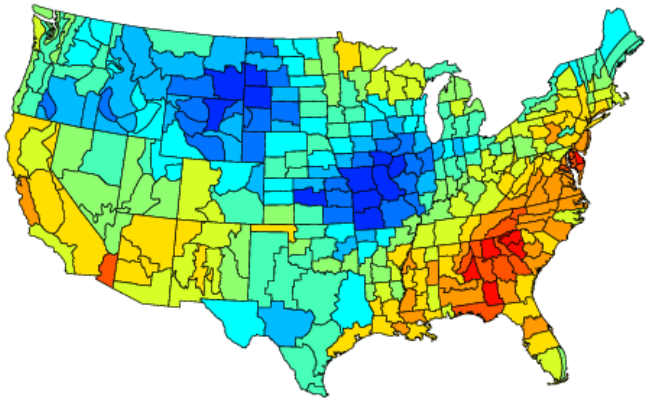

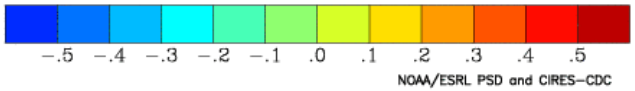

1981-2010

Divisional Precipitation Correlations with AMO

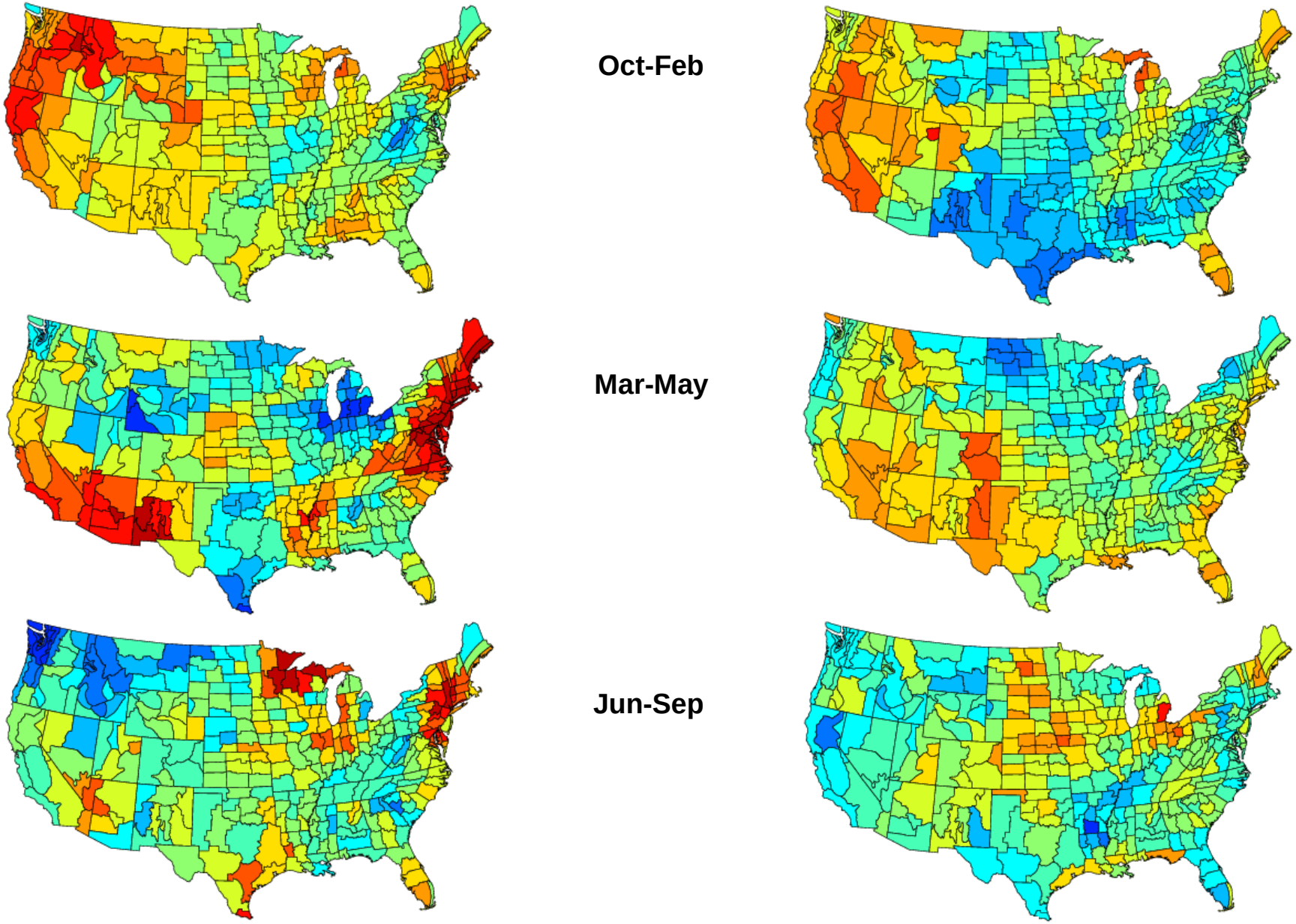

A13

1948-1964

1965-1990

APPENDIX B

References and Sources for Indices and Climate Data

Aleutian Low
Beamish, R.J. and D.R. Bouillon 1993. Pacific salmon production trends in relation to climate. Canadian Journal of Fish and Aquatic Science 50, 1002–1016.

http://www.pac.dfo-mpo.gc.ca/science/species-especes/climatology-ie/cori-irco/alpi/index-eng.htm

Atlantic Multidecadal Oscillation
Enfield, D.B., A.M. Mestas-Nunez, and P.J. Trimble, 2001. The Atlantic Multidecadal Oscillation and Its Relation to Rainfall and River Flows in the Continental U.S. Geophysical Research Letters 28, 2077-2080.

http://www.esrl.noaa.gov/psd/data/timeseries/AMO/

Nino 3.4: Climate Prediction Center: http://www.cpc.ncep.noaa.gov/data/indices/

North Pacific Index
Trenberth K. and J. Hurrell, 1994. Decadal atmospheric-ocean variations in the Pacific. Climate Dynamics 9, 303-319.

http://climatedataguide.ucar.edu/guidance/north-pacific-index-npi-trenberth-and-hurrell-monthly-and-winter

Northern Atlantic Oscillation, **Pacific North American pattern**
Wallace, J.M. and D.S. Gutzler, 1981. Teleconnections in the geopotential height field during the Northern Hemisphere Winter. Monthly Weather Review 109, 784-812)
Arctic Oscillation
Thompson, DW.J. and J.M. Wallace, 1998. The Arctic Oscillation signature in the wintertime geopotential height and temperature fields. Geophysical Research Letters 25,1297-1300.

http://www.cpc.ncep.noaa.gov/products/precip/CWlink/daily_ao_index/teleconnections.shtml
(link is flakey - keep trying)

Pacific Decadal Oscillation
Mantua, N.J. et al. 1997. A Pacific interdecadal climate oscillation with impacts on salmon production. Bulletin of the American Meteorological Society 78, 1069-1079.
http://www.atmos.washington.edu/~mantua/abst.PDO.html

Precipitation and temperature and climate data maps for the western US were obtained from WestMap Climate Analysis & Mapping Toolbox: http://www.cefa.dri.edu/Westmap/

West Map data original from PRISM (Daly et al. 2008)

Sea Surface Temperatures, 500mb, and Division climate data images provided by the NOAA/ESRL Physical Sciences Division, Boulder Colorado from their Web site at http://www.esrl.noaa.gov/psd/

Plotting and analysis: http://www.esrl.noaa.gov/psd/cgi-bin/data/getpage.pl

APPENDIX C

North American Drought Dipole and its Influence on Colorado River Flow

(Annotated Presentation from AGU 2010)

Separate PowerPoint file: AppendixC.pptx

APPENDIX D

Characterizing and visualizing drought onset for the Colorado River

S. Brewster Malevich
University of Arizona
malevich@email.arizona.edu

Introduction

The analysis presented in this paper briefly explores patterns in drought onset in the natural water year streamflow of the Colorado River. This addresses concerns about the relationship between flow sequences during drought and the impact these sequences have on reservoir storage. More specifically I hope to explore the following questions: Are there general characteristic of flow departures and duration that apply? What are the exceptions, and can we use these to identify flow sequences that have a particularly severe impact on reservoir storage?

Methods

Data

This report uses two series of natural streamflow data for the Colorado River at Lees Ferry, Arizona. The first series is a stream gauge record from water year 1906 - 2010, with 2008 - 2010 values based on streamflow estimates (Russell Callejo, personal communication). The second series is a tree-ring based reconstruction of Lees Ferry natural flow (Meko et al. 2007), extending from water year 762 - 2005. The reconstruction allows for an assessment of drought characteristics beyond those contained in the relatively short gage record.

Droughts and drought characteristics defined

Drought events are identified in each of the series. The characteristics of these droughts are then defined. These characteristics include starting year, duration and drought “intensity”.

A drought is defined as years of below-average streamflow, broken by two or more consecutive years of above average flow. This definition allows a wide range of hydroclimatic extreme events to be taken into consideration. With this definition, twelve droughts in the gage record and 169 in the reconstructed record were identified. Between the two records, 84 of the identified droughts are four years or longer in duration.

For this report, drought duration is the number of years of the drought (as defined above). A given drought event's intensity is simply the sum of departures from the respective series mean, for the given drought years.

Drought intensity and duration are significantly correlated (Pearsons; $\alpha = 0.05$; $p > 0.005$) at $r = -0.91$ and $r = -0.80$ for gauge and reconstruction record droughts, respectfully. These measures are negatively correlated because longer drought intensity corresponds to a greater negative cumulative departure.

Assessment of drought impacts using a simple reservoir model

The annual streamflow for each individual drought is run through a simple, dynamic model based on Lake Powell, for the first four years of each drought event. This analysis is limited to the first four years of each drought because in the gauge record a longer run of years would cause model runs to contain multiple drought events, and thus risk over representing certain portions of the streamflow series. The focus of this method is on the relatively short-term response to drought.

The simple model use here (Fig. 1) removes the influence of water demand and management, using initial reservoir-storage, plus inflow from the Colorado at Lees Ferry, minus

"down-stream allocations", and the desired number of simulated years as input variables. This modeled reservoir has no limit in storage.

The purpose of this simulation is not strictly to understand reservoir behavior (best explored using the CRSS model). Instead, this toy model acts as a sandbox to standardize and initialize drought events; allowing a more even comparison between the streamflow within different droughts, particularly as the effect of drought onset compounds, or alleviates stress over consecutive years. Similar results could likely be produced by using a series of cumulative streamflow, as it is the relationship between patterns of consecutive streamflow years which are of interest. However, a simple toy model is used because we are exploring a process or system. The model helps us to easily approach, understand and communicate this as a system problem.

Analysis in this report is performed with R (R Development Core Team 2011). The tools and code used in this report are freely available online[1] under an open source license.

Results

Select droughts identified from the stream gauge and streamflow reconstruction are shown in Tables 1 and 2, respectively. When compared, the droughts from these two series suggest that the general relationship between drought duration and intensity may be well represented in the reconstruction (Fig. 2). Note that because of the way drought is defined, it is possible to have small positive intensity values for relatively short droughts (such as the early 20th century) that are broken by a very wet single year, once or twice within the defined drought period.

[1] `https://code.launchpad.net/~brews/+junk/USBR_drought_onset_report_2011`

The reservoir simulations based on gauge record droughts (Fig. 3) show relatively little variation in reservoir storage for the initializing year of the model runs. An increasingly wider variation in reservoir storage is exhibited by the simulations by the third and fourth years of the model runs. In general, this variation comes from model runs with short-duration droughts (i.e., one to three years) which have higher reservoir storage at the end of the four-year onset period, since there has been some recovery. On the other hand, the longer-duration droughts are still experiencing drought, at the end of the onset period. The individual exceptions to this generality reflect the differences in intensity of these drought over the first four years of the event. For example, the short drought identified in 1919 cause reservoir storage to explode as the four year simulation runs into high flows of the 1920's.

The simulations based on the reconstructed droughts (Fig. 4) show a similar pattern to the droughts found in the gauge record. In general, there is largely the same progression in short- and moderate-duration droughts that we find in the gauge record. The distribution, however, has been greatly fleshed-out as a consequence of the 157 additional droughts found in the reconstruction record. Interestingly, a two-sided t-test suggests that the mean impact of longer-term, sustained droughts (8 - 25 year; $n = 22$) captured by the reconstructed record do not differ significantly when compared with the mean impact of moderate duration droughts (3 - 7 year; $n = 56$) by the end of the four year simulation periods ($\alpha = 0.05$; $p = 0.163$). This suggests there is no difference with respect to the sequences of flows in the first four years of the record's drought events.

Discussion and Conclusions

One of the first things to note, as mentioned above, is that the toy reservoir fills rapidly, quickly surpassing the actual storage of Lake Powell. Regardless, the effect that drought events have in the simulation is rarely a decrease in reservoir storage, but more often, a decrease in the rate with which the simulated reservoir fills. This would suggests an almost rainbow-like pattern where, in general, reservoir storage holds, or slowly climbs and then gradually returns to a non-drought fill-rate as the drought event subsides. Thus, we see differentiation in storage distribution after the model has passed a given drought's stopping-year. This explains why there is a stronger differentiation in the simulation runs between short-term droughts, when compared with moderate- and long-term droughts; in other words, the short-term droughts had expired during the model run.

The results from reconstructed drought simulations suggest that droughts of varying duration are generally indistinguishable from one-another during the four-year onset period. The same can be said for drought intensity, as the two characteristics are strongly correlated with one-another.

Averaging drought intensity over drought duration (Fig. 5) suggests that the average annual intensity of the longest droughts (which have the greatest cumulative intensity) tend not to be unusually strong. Shorter droughts, due to higher number of such events and through lower duration, have a wide range of annual average intensity values.

A next step could be to examine outlying events, and patterns with strong average annual intensity and high cumulative intensity, such 1845 through 1847, and the events of the past decade, to identify hydroclimatic conditions and mechanisms that accompany these droughts.

Aside from examining select droughts, it may be beneficial to systematically look at the range and variance of streamflow values within drought events in order to identify short bursts of sustained strong low flow, or the opposite case: sustained moderate low flow. Using the simple technique used in this report, this information on variability could then be combined with the existing drought characteristics and used in cluster analysis. It is possible that patterns will appear in the onset simulation runs if we categorize data based on these combined-variable clusters.

Acknowledgements

This work was informed by discussions with Kiyomi Morino and Connie Woodhouse

Table 1. Drought events identified in the Lees Ferry gauge record (1906 - 2010) which are four year duration or longer.

start year	stop year	duration (years)	intensity (AF)	average annual intensity (AF)
2000	2010	11	-33,132,829	-3,012,075
1959	1969	11	-25,783,066	-2,343,915
1931	1940	10	-24,868,066	-2,486,807
1988	1996	9	-16,773,649	-1,863,738
1950	1956	7	-17,247,402	-2,463,916
1972	1977	6	-10,229,108	-1,704,852
1943	1946	4	-5,786,947	-1,446,737

Table 2. Droughts over eight years in duration as identified in the Meko et al. (2007) Lees Ferry tree-ring reconstruction (762 - 2005).

start year	stop year	duration (years)	intensity (AF)	average annual intensity (AF)
1273	1297	25	-43,253,746	-1,730,150
1144	1158	15	-36,388,248	-2,425,883
1035	1049	15	-19,698,248	-1,313,217
1411	1425	15	-17,758,248	-1,183,883
1658	1671	14	-27,423,698	-1,958,836
1770	1782	13	-25,889,148	-1,991,473
1165	1177	13	-22,159,148	-1,704,550
1397	1407	11	-13,890,048	-1,262,732
975	984	10	-26,335,498	-2,633,550
1874	1883	10	-25,375,498	-2,537,550
1066	1075	10	-23,805,498	-2,380,550
901	910	10	-17,865,498	-1,786,550
1801	1810	10	-12,265,498	-1,226,550
822	830	9	-27,500,949	-3,055,661
1579	1587	9	-26,680,949	-2,964,550
1442	1450	9	-18,560,949	-2,062,328
949	957	9	-17,160,949	-1,906,772
933	941	9	-7,970,949	-885,661
1335	1343	9	-4,290,949	-476,772
1818	1825	8	-18,016,399	-2,252,050
860	867	8	-17,296,399	-2,162,050
812	819	8	-17,046,399	-2,130,800

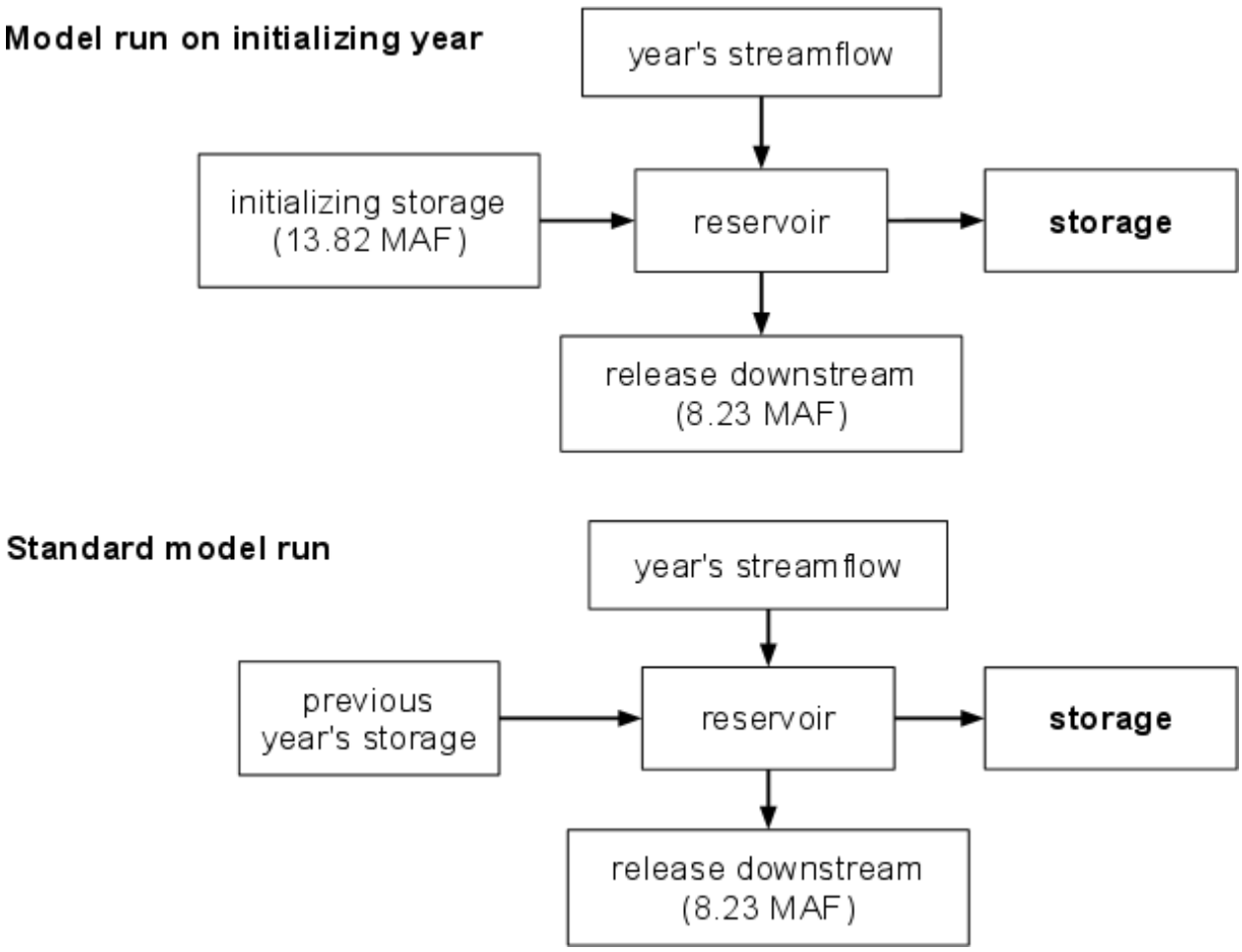

Figure 1. Toy model reservoir for accumulating streamflow based on Lake Powell. In the first year of a simulation, that year's streamflow is added to an initializing storage, a portion of this water is subtracted as it is "released downstream". The result is storage for the initializing first year of the simulation. This storage value is then added to the next year's streamflow and an amount is released downstream. The result of this is then stored for next year, and so forth.

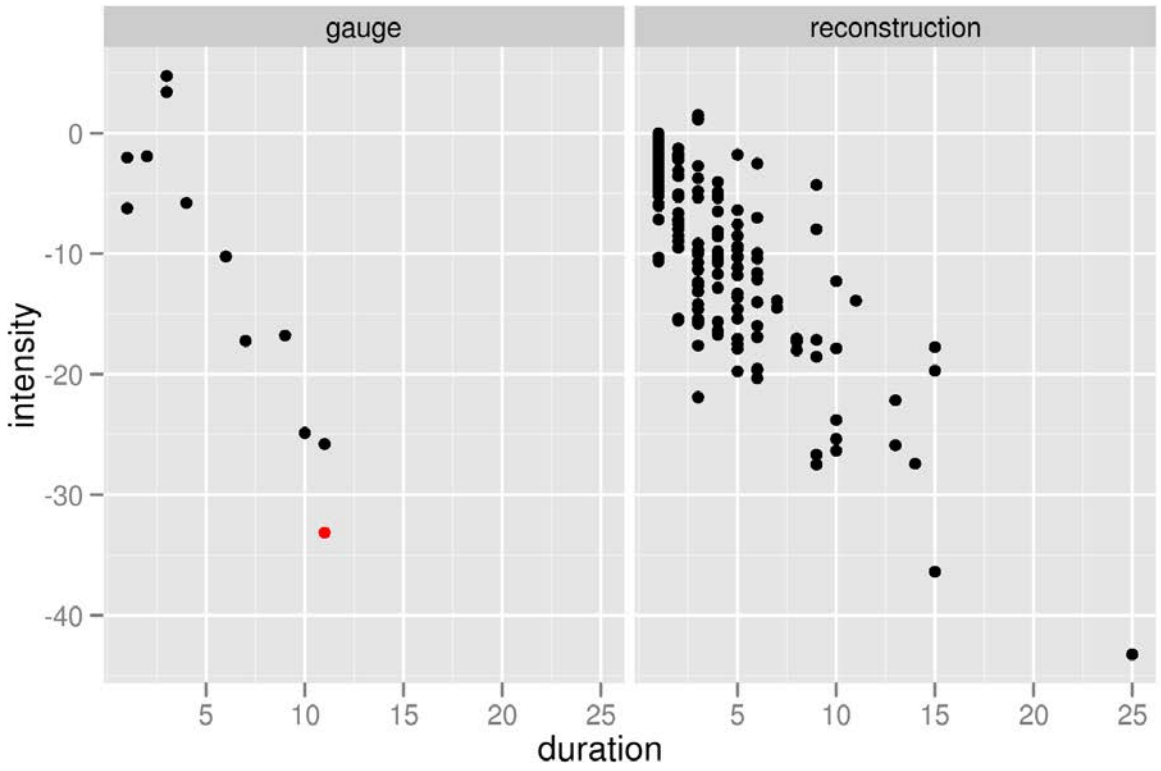

Figure 2. Comparison of drought characteristics as identified in the gauge and reconstructed records. The reconstruction appears to adequately recreate the relationship found in the gauge record. Note that the observation for the 2000 - 2010 drought is identified in red. This drought is not fully captured in the reconstructed record, which ends in 2005.

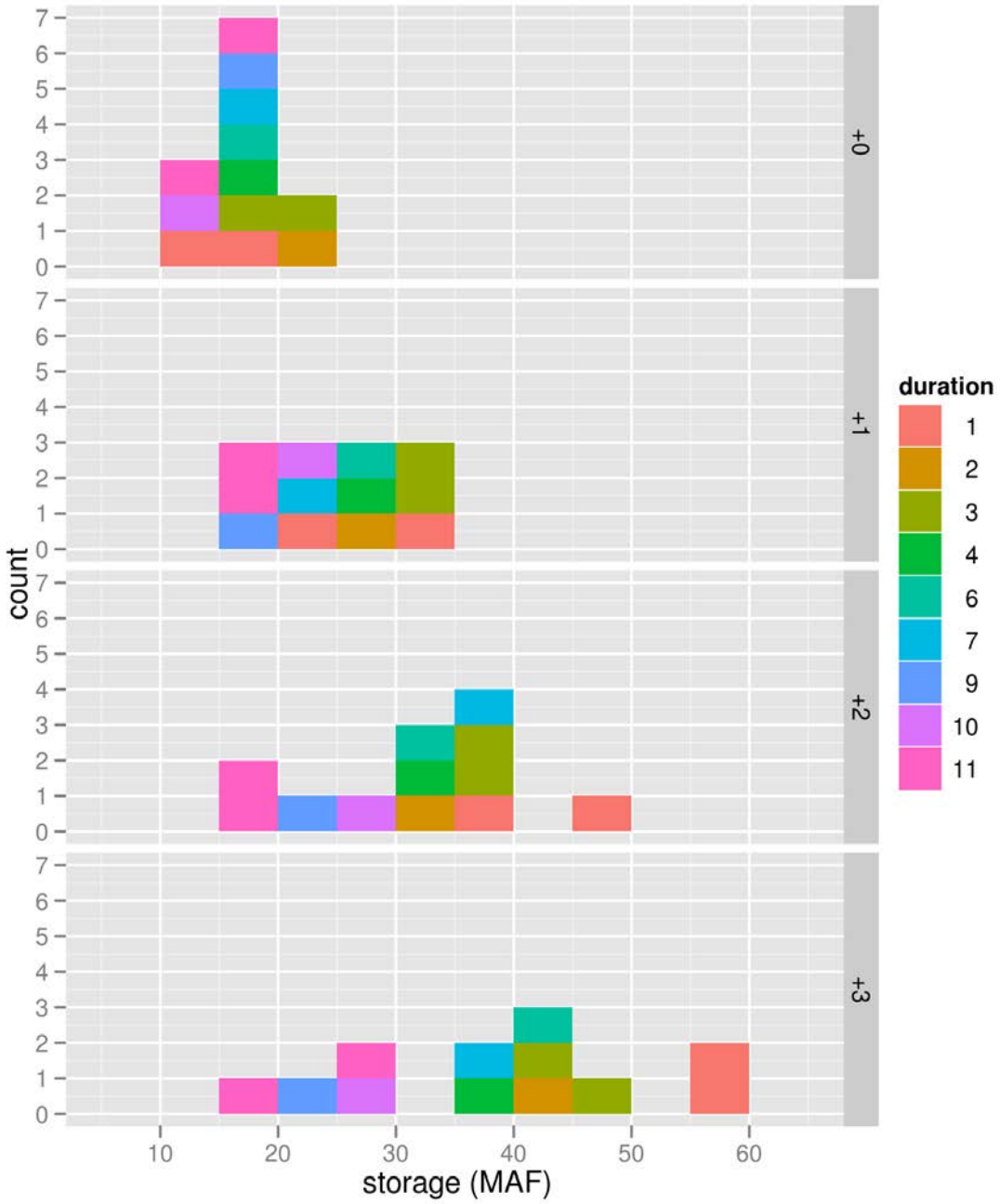

Figure 3. Simulations of droughts identified in the Lees Ferry gauge record. Histograms are stacked upon one another to show how the distribution of reservoir storage evolves over time, through the onset different drought events. The top histogram ("+0") is the first, initializing year of the independent simulations. The bottom histogram ("+3") shows the same information after the simulations have run for four years. Each colored rectangle represents a single drought event, in the given simulation year. For example, there are seven droughts shown in the initializing year, which resulted in 15 - 20 MAF of reservoir storage. These seven droughts include one 11-, 9-, 7-, 6-, 4-, 3-, and 1-year droughts.

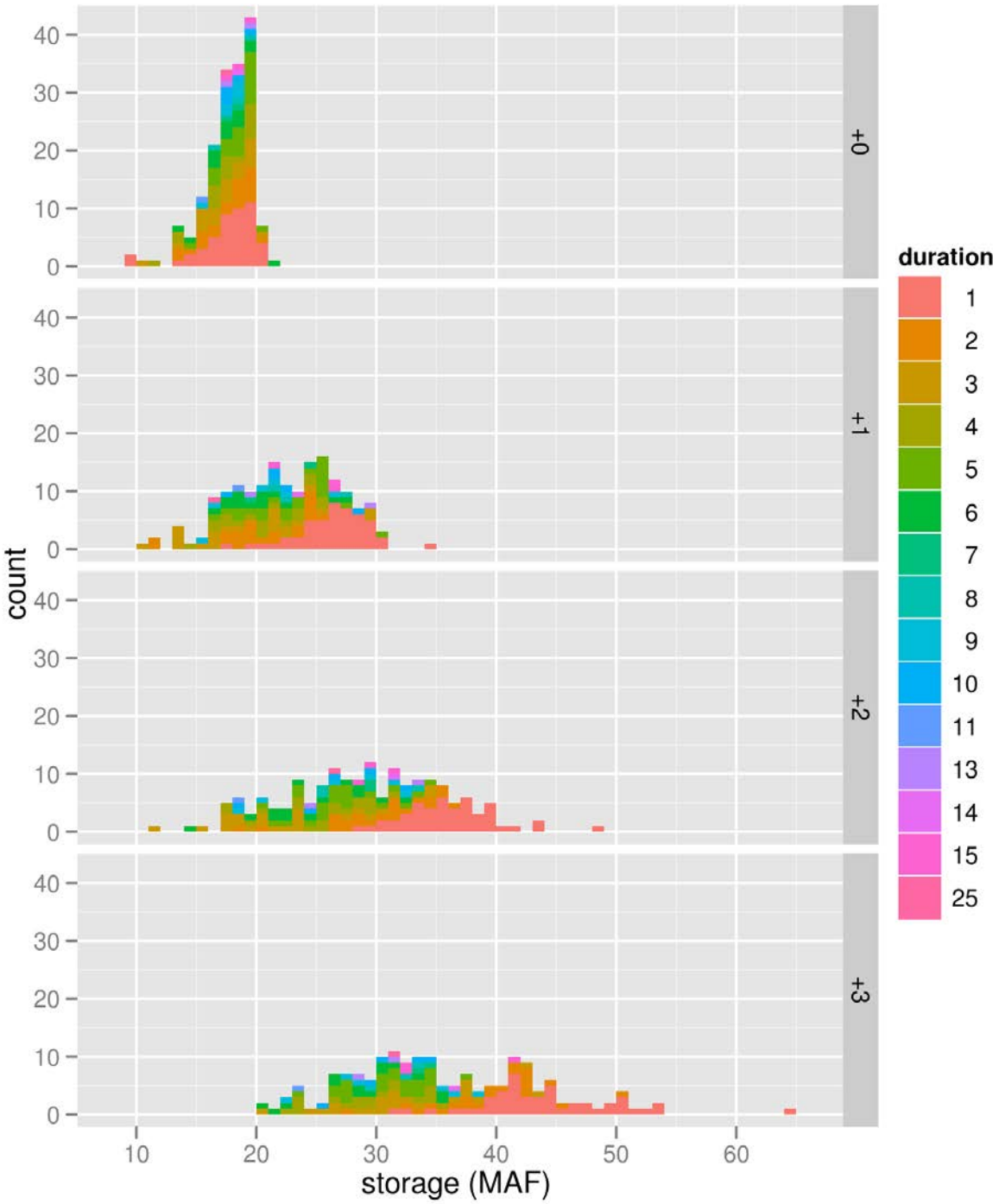

Figure 4. As in Fig. 3, instead using simulations of droughts identified in the Meko et al. (2007) tree-ring reconstruction of Lees Ferry streamflow. Note that with the higher sample size of the reconstruction, the distribution of long- and moderate- duration droughts is very similar through to the end of the four year onset period. A higher resolution 1-MAF bin size is used for these histograms as opposed to the 5-MAF bins in Fig. 3. There is a difference in short-term droughts and these droughts have, or are in the process of ending, and thus, the reservoir is allowed to recover.

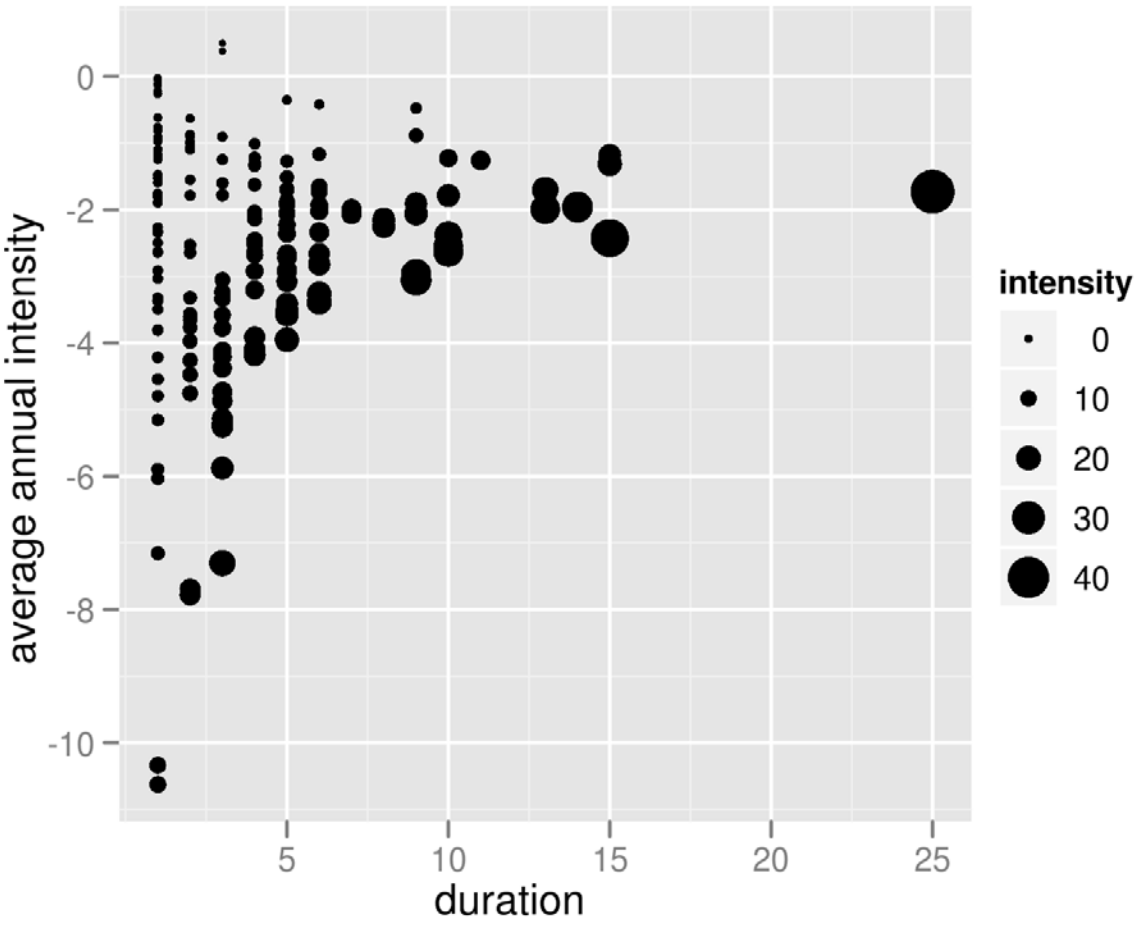

Figure 5. Relationship between characteristics for droughts identified in the Meko et al. (2007) Lees Ferry reconstruction. Moderate- and long-duration droughts do not necessarily contain the most intense, individual drought years - a consequence of the large sample size in these longer droughts.

References

Meko, David M., Connie A. Woodhouse, Christopher A. Baisan, Troy Knight, Jeffrey J. Lukas, Malcolm K. Hughes, and Matthew W. Salzer. 2007. “Medieval drought in the upper Colorado River Basin.” *Geophysical Research Letters* 34 (10) (May). doi:10.1029/2007GL029988.

R Development Core Team. 2011. *R: A language and environment for statistical computing.* Vienna, Austria: R Foundation for Statistical Computing. http://www.R-project.org.